Orientations of galaxies and their distribution in space

Edalati, M.T.

ORIENTATIONS OF GALAXIES AND THEIR DISTRIBUTION IN SPACE

A thesis submitted to the University of Durham

for the degree of Master of Science

by

M.T.Edalati, B.Sc. (Iran)

December 1976

To Mehdi,

My brother

ABSTRACT

Distributions of angular momenta of galaxies can be used to test theories of galaxy origin. The observational problems are discussed in detail. Previously, interpretations have been hampered by physical and physiological selection effects that operate on visual measurements. With the COSMOS machine and the deep Schmidt plates many of these problems should be overcome. Before investigating the COSMOS data, two visual sets of measures were examined. Firstly, Brown's original uncorrected catalogue of position angles was studied. Previous investigators claim remarkable anisotropies exist in this data, and indeed there are some histograms showing peaks significant at the 4σ-level. Further examination reveals little reason for considering these excesses to be physical, and, taking into consideration the number of histograms possible (by splitting the data with various parameters), the anisotropies are too insignificant to use in theoretical arguments.

Secondly, a set of visual measurements made on a deep UK Schmidt plate recording both position angles and axis ratios was examined. The position angles are consistent with that expected for a random distribution, except for the smallest galaxies where some selection effect may be involved. There is no evidence for a correlation between position angles of adjacent galaxies. When the quantization effects are taken into account the axial ratio distributions are consistent with a random 3-dimensional orientation of a mixture of 83 % spirals and 17 % ellipticals. A comparison of the distribution of nearest neighbour separations with that expected for a random distribution of galaxies on the sky shows that there is clustering . When combined with an estimate of the size of clusters

from a covariance analysis a mean number of 6.5 galaxies per cluster is obtained.

Using COSMOS coarse mode measurements of a portion of plate R1049, galaxy axial ratio distributions have been obtained. The results can not be explained by any mixture of galaxy types. To check COSMOS, the plate was scanned by eye and an assessment of the machine is provided. At the intermediate sizes $100\,\mu m < 2a < 200\,\mu m$ the identifications are satisfactory, but for larger images there are unexplained errors in the COSMOS data. For both sizes the agreement between the axial ratios from COSMOS and those measured by eye is disappointing. It is concluded that further work of this nature must be performed only using the fine-mode facilities of the machine.

PREFACE

The work described in this thesis was carried out during the period September 1975 to December 1976, while the author was a research student under the supervision of Dr. J.L.Osborne in the Physics Department of the University of Durham .

CONTENTS

CHAPTER 1

INTRODUCTION

1.1 - General remarks

One of the outstanding problems in the study of galaxy formation is the origin of the angular momentum of galaxies. There are currently two opposing theories for the origin of the galaxies (see Jones 1976 for an excellent review of the subject), namely the gravitational instability theory (Peebles, 1970) and the cosmic turbulence theory (Ozernoi, 1974) . In the latter theory the angular momentum is naturally explained as a result of the turbulent eddies, but some difficulty has been encountered in explaining the observed angular momentum of spiral galaxies in the context of the gravitational instability theory. Here the spin is supposedly caused by tidal forces induced by motions of adjacent galaxies.

Most of the slow progress in this field is caused by a lack of observational results especially those relating to the angular momenta of galaxies. The main aim of this thesis is to collect data on the distribution of angular momenta, and to investigate whether there is any non-randomness in these distributions. Such anisotropies, if they exist, could further our understanding of the origin of galaxies.

It is not possible to determine the specific angular momentum of a galaxy without detailed studies of the stars that constitute it. In order to investigate the distribution of angular momentum for many galaxies, we must therefore resort to allied quantities such as apparent shapes and orientations. It is then necessary to make assumptions about the true shapes of galaxies and the direction of the angular momentum vector in the frame of the galaxy.

From the few detailed observations of nearby galaxies it seems reasonable to assume that the angular momentum vector is aligned parallel to the true minor axis of the galaxy. The situation concerning elliptical

galaxies is still not clear, and where the distinction can be made, we will deal with spirals only. With the above assumption we can test for anisotropy by studying the orientations and shapes of many galaxies. We now define the necessary observable quantities.

Position angle

The position angle of a galaxy is the angle measured counterclockwise from some fixed direction (normally due north) to the line defined by the intersection of the plane of the galaxy with the plane of the sky; that is the angle between the meridian passing through the object and the direction of its apparent maximum diameter (major axis) measured from north through east (see figure 1) . Position angles are readily obtained for all galaxies except those whose images are nearly circular and those that are not elliptical in apparent shape.

a : Semi major axis

b : Semi minor axis

φ : Position angle

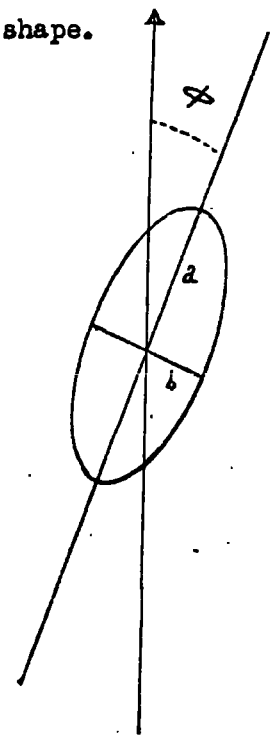

Fig. 1

Inclination

This is simply the angle between the plane of the galaxy and the line of sight, and an estimate of the inclination can be found from the apparent flattening of a galaxy if the true shape is known.

b : Apparent semi minor axis

B : True semi minor axis

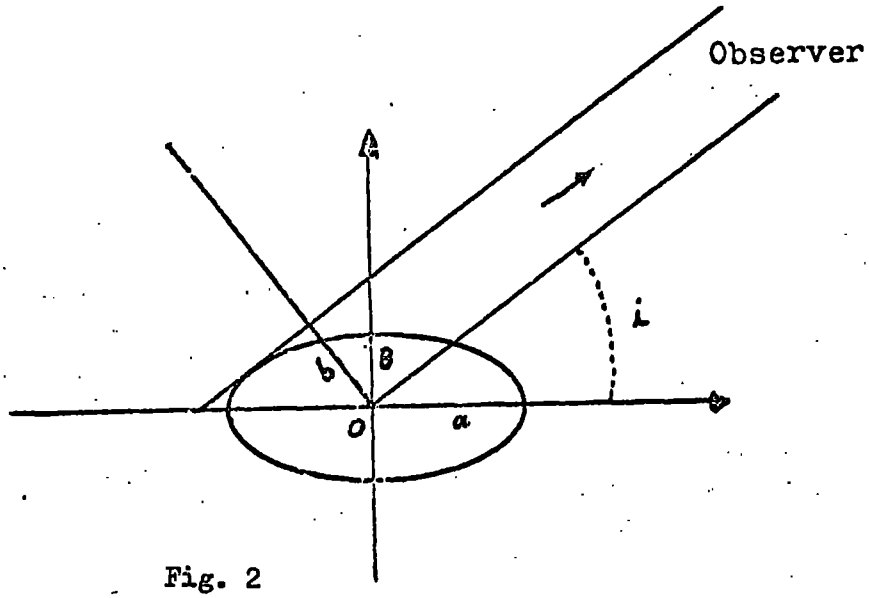

Fig. 2

Axial ratio

The axial ratio is defined by the ratio of semi minor axis (b) to semi major axis (a). The amount of inclination can be roughly found from measures of b/a . In the simple case where a galaxy is a thin circular disk, the inclination is given by :

$$\text{Cos } i = b/a \qquad \text{(see figure 2)}$$

The distribution of apparent axial ratios for elliptical, S0+SB0 and ordinary spiral galaxies confirm that the ellipticals have only moderate intrinsic flattening whereas ordinary spirals and S0's are intrinsically flatter, possessing thin disks with little dispersion in thickness (Sandage et al. 1970) . In principle the frequency function of true axis ratios of spheroidal galaxies can be derived easily from the observed frequency function of apparent axial ratio under the assumption of random orientation of the angular momentum. This problem has been often treated, mainly with respect to elliptical and lenticular (S0) galaxies. Later we will analyse this problem for two different data sources (measured by hand and by machine) and the inclination in the general case will be discussed then. It should be pointed out, however, that position angles and inclinations can not determine

the direction of the angular momentum absolutely; in fact these parameters give four possible orientations, since we can not distinguish between opposite senses of spin and there is also a geometrical ambiguity.

1.2 - Description of the Data

In this research work, we have used three different types of data as follows :

a - Brown's measurements (Brown, 1964, 1968)

The only available data on orientation angles for large samples of galaxies are those measured by Brown (1964, 1968).
He determined position angles and axis ratios for more than 9000 galaxies on the blue and red prints of the Palomar Sky Survey in the constellations Pisces, Virgo, Ursa-Major, Hydra and Eridanus.
Dr. Brown kindly supplied his original measurements which are, for each galaxy :
the position (X and Y) on each plate, the maximum angular diameter, the form (axial ratio) and the orientation angle. We have selected from this data only the spiral galaxies.
In the first set of measurements (Brown, 1964) position angles were listed for all galaxies omitting a value only for images that were nearly circular ($b/a > 0.75$) . Later however, this limit was reduced to 0.55 since Brown felt that for $b/a > 0.55$ position angles were uncertain. This data and its treatment is discussed thoroughly in chapter 2.

b - ROE data

The ROE (Royal Observatory Edinburgh) data, is a catalogue of 3054 galaxies compiled by Professor Reddish from a IIIaJ Schmidt plate in an area of 2 square degrees near the south galactic pole. The data consists of the positions, sizes (diameters) shapes and orientations.

Spirals and ellipticals are not distinguished in this data . It is estimated that the galaxies observed are distributed to distances corresponding to redshifts of about 0.5 (Dodd et al. 1975).

We have analysed this data to examine the distribution of orientation angles of all galaxies, the distribution of the difference between orientation angles of nearest neighbour galaxies, the distribution of axial ratios of spirals and ellipticals, clustering and also the ratio of spirals to ellipticals. The results are given in chapter 3.

c - COSMOS data

COSMOS is a sophisticated machine (Pratt et al. 1975) capable of precision measurement of co-ordinates, size, magnitude, orientations and shapes of astronomical images.

Essentially the machine is a rapid scanning densitometer which analyses individual images above a certain threshold. A detailed description of COSMOS has been given by MacGillivray (1975) and we reproduce in table 1 the main description of this facility.

This thesis is concerned with the measurements by COSMOS of deep Schmidt plates taken on the UK 48-inch Schmidt Telescope at Siding Spring, Australia. The specific details of these data and the results of the distributions of axial ratios and nearest neighbour galaxies are provided in chapter 4.

Table 1

COSMOS

Photographic plate size: up to 356mm X 356mm

Plate carriage:	moved hydraulically and positioned by a transmission grating system to $\pm 0.5 \mu m$.
Scanning systems:	two independent microspot cathode ray tubes, one giving a raster scan, the other a spiral scan.
Machine control:	general purpose mini-computer with 8192 words of 16 bit storage.
Machine output:	machine tape deck of 1600 bits per inch, 75 inches per second.
Raster scan systems:	Spot sizes of 8, 16 or $32 \mu m$ with corresponding lane widths of 1, 2 or 4mm respectively; for the $8 \mu m$ spot the scanning rate is 2 square mm per second, or one full-sized plate per day ; transmission digitised to 127 levels.
Spiral scan system:	three magnifications give field scanning diameters on the plate of 256, 820 and $2048 \mu m$ respectively, generates family of 1024 general ellipses, centres on image and determines best fitting ellipse.

1.3 - Comments on the distribution of angular momentum of galaxies

Possible anisotropies in the distribution of angular momenta of galaxies have been discussed by many astronomers.

Brown (1938) claimed he had found evidence for anisotropy in Shapley's catalogue that contains 7,889 external galaxies in the Horologium region. He also found that the frequency function of position angles for an area close to the south galactic cap lying chiefly in Cetus (Wyatt and Brown, 1955) and partly in Pisces (Brown, 1964) was markedly skew.

The Cetus measurements were repeated by Kristian (1967) independently, and he used different plate material; nevertheless, his results did not confirm Brown's work, that is the distribution he obtained was flat. This discrepancy has not been resolved.

Reaves (1958) also did not accept Brown's result, therefore he scanned position angles of galaxies on two plates covering part of the region of the Shapley survey and found no evidence for anisotropy.

Reinhardt (1971, 1973) however, agrees with Brown's comments and says that there are statistically significant departures from isotropy indicating a non-random distribution of angular momenta.
He adds that it is difficult to ascribe these departures (Brown's results) to selection effects, because Brown finds preferences for more than one angle.

Opik (1969) argued that Brown's observations may be subject to systematic observing errors. Opik emphasized that the accuracy of Brown's measurements and care of his investigation is not questioned, but that there is possible unconscious bias in the selection of galaxies. He suggested that plates should be measured in two distinct orientations.

Brown did this for three plates of the Pisces region but found no significant differences. However, Hawley and Peebles(1975) add that Opik had suggested that the two catalogues should be compiled independently,

whereas Brown simply remeasured one catalogue.

1.4 - Selection effects

In considering position angles and axis ratios of galaxies, there are several unavoidable human and physical selection effects which must be discussed. These effects will be greatly simplified with the advent of COSMOS data; some will be eliminated altogether whilst the remaining effects will be reproducible and can be corrected for. In the following, we explain several kinds of selection effects and later we will consider their effects on the distribution of position angles and axial ratios in our data.

1- Holmberg effects

Holmberg (1946) in comparing photometric dimensions of synthetic galaxy images in his laboratory experiments encountered the following physiological effects :

a - First Holmberg effect :

This effect consists of a systematic underestimate of the axial ratio, the deviance being larger for edge-on galaxies (i.e. those with small axis ratios). The effect is not very dangerous, because it only redistributes according to inclination in a catalogue.

b - Second Holmberg effect :

This effect consists of an underestimate of the maximum diameter (major axis) by an amount which depends on the axial ratio. The deviance is largest for face-on galaxies. In considering this effect one must be very careful, because it causes incompleteness in catalogues listing galaxies down to a fixed limiting apparent maximum diameter. The second Holmberg effect is partly physiological but is mainly due to the visual effect of the intensity distribution across galaxies. One must be extremely careful therefore, in estimating distances from angular diameters. Isophotal diameter must first be corrected to their "face-on" equivalents and then corrected again before comparing with a 'true' metric size.

2- Selection effect by surface brightness (Opik effect)

This effect was discovered by Reynolds(1920) and was explained by Opik (1923) as follows.

Galaxies have greater surface brightness at small inclinations. For further discussion we can say if we consider two similar transparent galaxies at the same distance, one edge-on and one face-on, the radiation from the edge-on galaxy will emanate from a smaller angular area and thus its surface brightness will be enhanced. It means that at a fixed angular diameter limit, these edge-on images appear too frequently.

In the case of spirals, the effect is offset to some extent by the increased dust absorption and this renders the correction somewhat uncertain.

3- Quantization effect

All measurements(positions, major and minor axes of galaxies) in ROE data have been quantized. The X and Y coordinates are given to the nearest 254 μm(0.01 inch). The major and minor axes are given to the nearest 10 μm.

This effect is also present in COSMOS data (both position and extents are given in the nearest 8 μm), but as we shall consider only the larger galaxies for that data we can ignore the effect in the COSMOS observations and apply corrections only for the ROE data.

CHAPTER 2

Analysis of Brown's data

2.1- The need for another analysis of Brown's data

Brown's data have been studied by many investigators, but in all cases the result were taken from histograms given in his papers (Brown, 1938, 1964 1968, Wyatt, et al. 1955). It is important, however, to mention that Brown actually smoothed these true histograms before presenting them in his paper (Brown, 1968) , thus making conclusions about anisotropy rather dubious.

We have, by kind permission of Dr.Brown, been able to computerise Brown's original uncorrected measurements and thus we can investigate effects of smoothing and anisotropy on the genuine data. In particular, we are now able to correct each datum point (if required) for physical and physiological selection effects and to produce many more histograms for a variety of parameters (forms, diameters, etc.).

2.2- Description of the raw data

The original measurements under discussion have been described in detail by Brown (1964) and the catalogue is simply the raw uncorrected measurements grouped according to plate number and region of the sky. The galaxies are situated in an extensive area in the southern galactic hemisphere, centred in the constellation of Pisces; also in the northern galactic hemisphere centred in Virgo, Hydra and Ursa-Major. The measurements were made from prints of the National Geographic Society-Palomar Observatory Sky Survey. Each plate covers a maximum area of 36 square degrees, excluding overlap. For each galaxy in the catalogue we have its position, maximum angular diameter (in arcsec.), form(axis ratio) and, for the spirals the position angle.

There are two possible classifications for the form (measured by the ratio of the apparent minor axis b to the apparent major axis a); Harvard

classification ($F_{Harvard}=10(1-b/a)$) and Brown's classification ($F_{Brown}=10(b/a)$).

In this work, the form was given in the Brown classification; eg., form 1 means : $0 \leqslant b/a \leqslant 0.15$, form 2 : $0.15 < b/a \leqslant 0.25$ etc. up to form 10 : $0.95 < b/a \leqslant 1.0$. Note that the intervals are not quite uniform.

In the first set of measurements (Brown, 1964) position angles are listed for all spiral galaxies omitting a value only for images that were nearly circular ($b/a > 0.75$). Later however, this limit was reduced to 0.55 since Brown felt that for $b/a > 0.55$ position angles were uncertain. As Opik (1970) has pointed out, in studying the angular momentum distribution this selection in b/a is unnecessary.

Circular objects have poorly defined position angles but the direction of the angular momentum is fairly well determined. To make the entire catalogue homogeneous however,we have also had to impose a limit $b/a \leqslant 0.55$ for the first set of measurements.

The data are summarised in table 2 which gives the constellation, total number of plates and the total number of galaxies recorded on those plates, down to a limiting major axis of $40''$.

Table II

Brown's data

Constellation	Total no. of plates	Total no. of galaxies
Pisces	87	2843
Hydra	9	717
Ursa-Major	7	1004
Virgo	6	544
Total	109	5108

Our catalogue lists only spiral galaxies. Although Brown recorded ellipticals, mainly for morphological investigations, he omitted them from his position angle histograms. Opik (1970) has shown that useful information can be extracted from b/a and position angles for a set of ellipticals. It is not clear, however whether ellipticals possess any angular momentum,

whereas with spirals the position is more favourable and furthermore, the range of metric diameters observed is much less than that for ellipticals. Consequently any limiting angular size will lead to a less ambiguous distance limit.

The lower limit of diameter was fixed by Brown strictly at 0.6mm(40 seconds of arc) for the Pisces measurements and at 0.54 mm (36 seconds of arc) for the other regions. Although, one can readily distinguish the form and position angle of smaller galaxies, to ensure reasonable completeness of the survey, he considered it desirable to stop at the stated limits.

The primary consideration of observations was made on prints reproduced from the plates taken in blue light. Prints from the red plates were sometimes used to decide whether a galaxy was a faint spiral or a spheroidal object, since the images of ellipticals were usually found to be relatively stronger on the red plate than on the blue. The transitional S0 types were not clearly separated from the elliptical and spiral forms. We included the S0 galaxies with the spirals, when their axis ratio was less than 0.3 .

2.3- Statistical analysis of smoothed and raw data

In his 1968 paper Brown wrote the following :

" In most cases a smoothing out of the minor irregularities is effected by transferring limiting position angles from the proper group of six (degrees) to the one above or next below." Thus he altered the histograms to make them smoother and so possibly created an interesting psychological problem. As we know, the eye judges "noise" in a distribution by the scatter from point to point, therefore because the minor irregularities have been suppressed the noise or statistical scatter appears to be small and the occasional large statistical fluctuations appear to be more significant. Below we define the chi-squared and autocorrelation tests which we will use to examine the implications of this smoothing.

a- Chi-square (χ^2) test

For the data listed in table 1 frequency distributions of position angles have been plotted(see for example figures 3 and 4).
We wish to test whether the observed distributions are consistent with the hypothesis of an isotropically random distribution.

A test which is often used to test the equivalence of a probability density function of sampled data to some theoretical isotropy of the histograms is based on the following formula :

$$\chi^2 = \sum_{i=1,n} \left\{ (N_i - N_0)^2 / N_i \right\}$$

where N_i is the count in the i^{th} angle bin (observed frequency) and N_0 is the mean of N_i (expected frequency) over the n=30 bins.
For a random isotropic distribution of position angles the expected value of χ^2 is close to ν (the number of degrees of freedom); in this case $\nu = 30 - 1 = 29$. In table II we have listed for each sample of smoothed and raw data two different values for the following :
N (number of galaxies in the histograms), χ^2 (Chi-square), $P(>\chi^2)$, the probability that in a random distribution χ^2 exceeds the observed value, and finally $C_\sigma = \frac{C}{\sqrt{n}}$ (the autocorrelation coefficient in terms of standard deviation, see below). The upper line refers to values derived from Brown's, smoothed histograms, whereas the lower line refers to the raw data.If the position angles were randomly distributed, the probabilities $P(>\chi^2)$ should be uniformly distributed from 0 to 1 , whereas 5 out of 10 for the unsmoothed data have $P(>\chi^2) < 0.01$.

b- Autocorrelation coefficients

This test measures the correlation between the numbers of galaxies in adjacent bins. In this respect it is therefore a sensitive measure of the lack of noise or ' smoothness ' of a histogram. The autocorrelation coefficient is defined as :

$$C = \sum_{i=1,n} \frac{(N_i - N_0)(N_{i+1} - N_0)}{N_0}$$

where :

N_0 = Average number of galaxies per bin.

N_i = Number of galaxies in i^{th} bin.

n = Number of bins.

If the position angles are randomly distributed, the expected value of the autocorrelation coefficient is zero. It is more convenient, however to quote the autocorrelation coefficient in terms of its standard deviation, as follows :

$$\frac{C}{\sigma} = \frac{C}{\sqrt{n}}$$

where n is the number of bins.

Table III

Statistical parameters for smoothed and raw data in Brown's catalogue. Upper and lower numbers refer to smoothed and raw data respectively.

AREA	FORM	SIZE (Arcsec)	N	χ^2	$P(>\chi^2)$	$C_\sigma = C/\sqrt{n}$
PISCES	1 - 2	40 - 64	346	39	0.09 ↓	4.38
			337	52	0.005 ↓	1.73
	3 - 5	40 - 64	249	23	0.78	2.74
			255	39	0.10	0.81
VIRGO	1 - 3	> 65	230	44	0.03 ↓	3.47
			233	49	0.01 ↓	2.594
	4 - 5	> 36	102	20	0.90	2.00
			103	34	0.24	-0.405
URSA-MAJOR	1 - 2	> 65	238	26	0.63	2.92
			222	29	0.47	1.855
	3 - 5	> 50	238	18	0.94 ↓	219
			212	49	0.01 ↓	0.539
	3 - 5	36 - 49	203	28	0.53	2.92
			199	29	0.47	1.155
HYDRA	1 - 2	> 65	146	26	0.63 ↓	2.19
			152	58	0.001 ↓	-0.76
	3 - 5	36 - 64	230	20	0.89	2.56
			230	35	0.20	1.111
	1 - 2	36 - 64	268	28	0.54 ↓	3.47
			270	49	0.01 ↓	0.73

From table 3 , for the χ^2 -test, we see that in five samples marked ↓ smoothing reduced the significance of the apparent non-randomness of the position angle distributions. For the remaining five samples $P(\chi^2)$ is increased or decreased by the smoothing but in both cases is consistent with a random distribution.

If we compare the different autocorrelation coefficients in table 3 we find that C_σ for the smoothed data is consistently higher by about 2σ.

The above tests give us some measure of the distortions introduced by smoothing. As expected the C_σ values are considerably changed, and most of the beautiful peaks in the Brown papers are probably pure manifestations of transferring data (by one bin). Nevertheless in table 3 we notice five histograms that appear significant at the 1% level, as determined by the χ^2-test, before smoothing i.e., in the raw catalogue. Two of these histograms, (hereafter referred to as 'remarkable ' histograms) are reproduced completely in figures 3 and 4 .Apart from these, there is nothing significantly above the 2σ level as determined by the autocorrelation test in the data .

We now turn our attention to these two histograms (in Virgo and Hydra) .

2.4 - Description of ' remarkable ' histograms

In the annexed histograms (figures 3 and 4), all spirals, down to the limiting diameter (65 arcsec) and forms (1-3, 1-2) over the whole of the 6 plates (for Virgo) and 9 plates (for Hydra), are binned at intervals of 6^0. The histograms refer to the raw data, but the raw and smoothed counts are written alongside.

Figure 3 shows that the position angles of spirals, and with axis ratios lying between 0 and 0.25 or form 1-2, show a strong preference for values near 36^0 and 120^0. It is interesting that the number of galaxies in these two peaks are the same for the smoothed data .

If we compare the number of galaxies in the raw data (figure 3) with the numbers in the smoothed data between position angles 36^0-42^0, we find that, there is little difference; in other words Brown's smoothing , in this case, has not changed the original histogram very much.

Figure 4 shows another ' remarkable ' histogram of position angles in Hydra region. Here there is a preference for values at 30^0-36^0 and 168^0-174^0. The number of galaxies in the first peak (30^0-36^0) is equal to that in Brown's paper, whereas in the second peak (168^0-174^0) the counts are different.

To examine the significance of these peaks their height in standard deviations above the mean can be calculated. In figures 3 and 4 the solid line shows the mean number of galaxies in a bin $\bar{n}$ while the dashed lines show the $\pm\sigma$ limits where the standard deviation $\sigma = (\bar{n})^{\frac{1}{2}}$. In figure 3 the peaks at 36^0-42^0, 126^0 - 132^0 are respectively 4.7σ and 1.9σ above the mean. In figure 4 those at 30^0-36^0 and 168^0-174^0 are 3.1σ and 4.4σ above the mean.

N_{raw}	N_{Brown}	$\phi°$
7	8	0
6	6	6
5	6	12
6	5	18
7	6	24
9	10	30
21	21	36
12	12	42
8	10	48
9	7	54
3	4	60
8	5	66
4	5	72
2	5	78
6	3	84
7	8	90
7	7	96
8	6	102
5	7	108
8	7	114
6	7	120
13	13	126
10	8	132
11	13	138
7	8	144
9	8	150
10	8	156
3	6	162
6	7	168
10	7	174

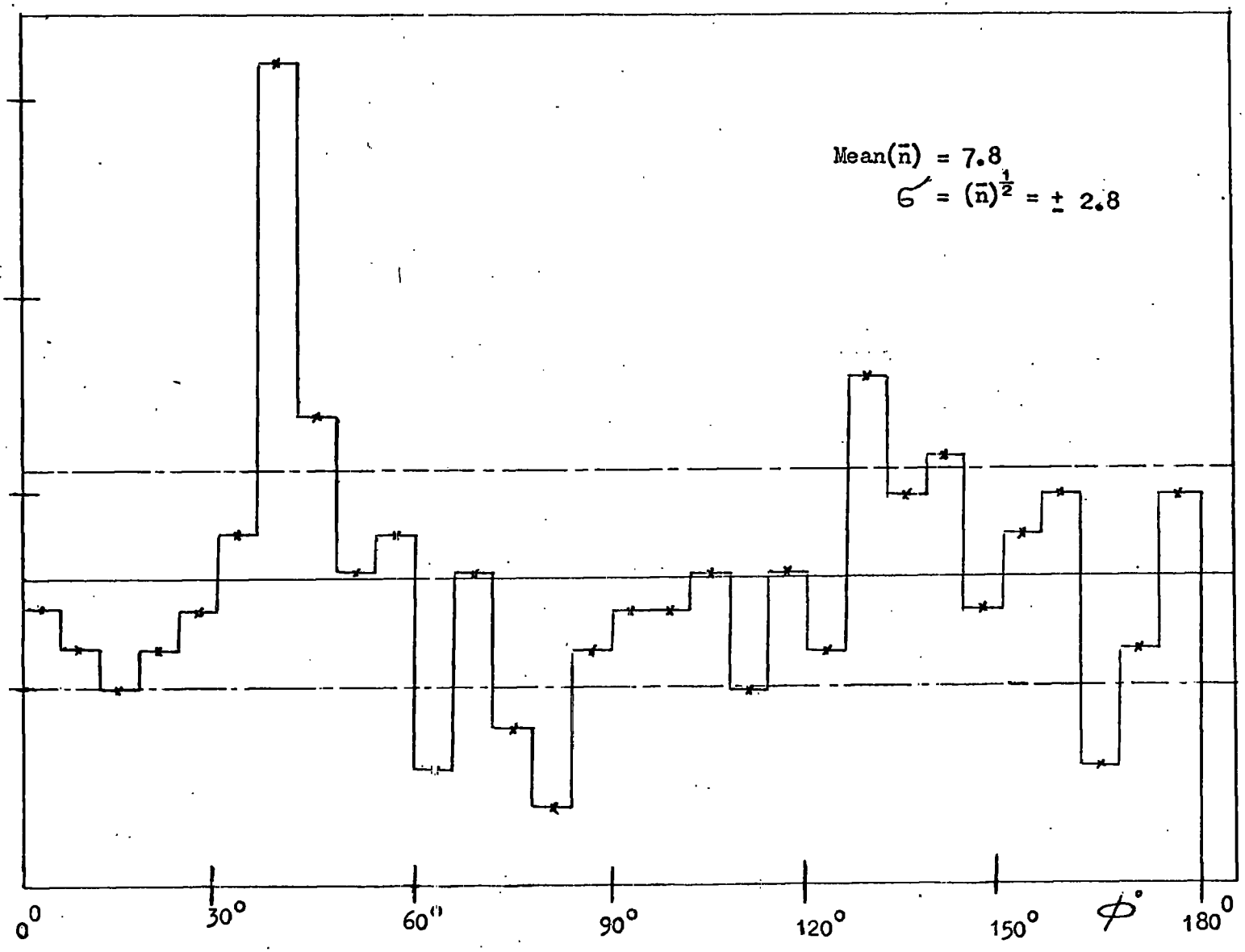

Fig. 3- Frequency function of galaxies against the position angle in Virgo (Raw data).

N_{raw}	N_{Brown}	ϕ^{o}
3	5	0
6	5	6
7	5	12
2	3	18
4	4	24
12	12	30
6	8	36
8	7	42
8	6	48
4	5	54
2	5	60
7	4	66
4	5	72
6	5	78
4	5	84
3	3	90
2	1	96
1	2	102
4	3	108
2	3	114
5	4	120
4	4	126
5	4	132
2	3	138
9	7	144
8	8	150
4	4	156
1	5	162
15	6	168
4	5	174

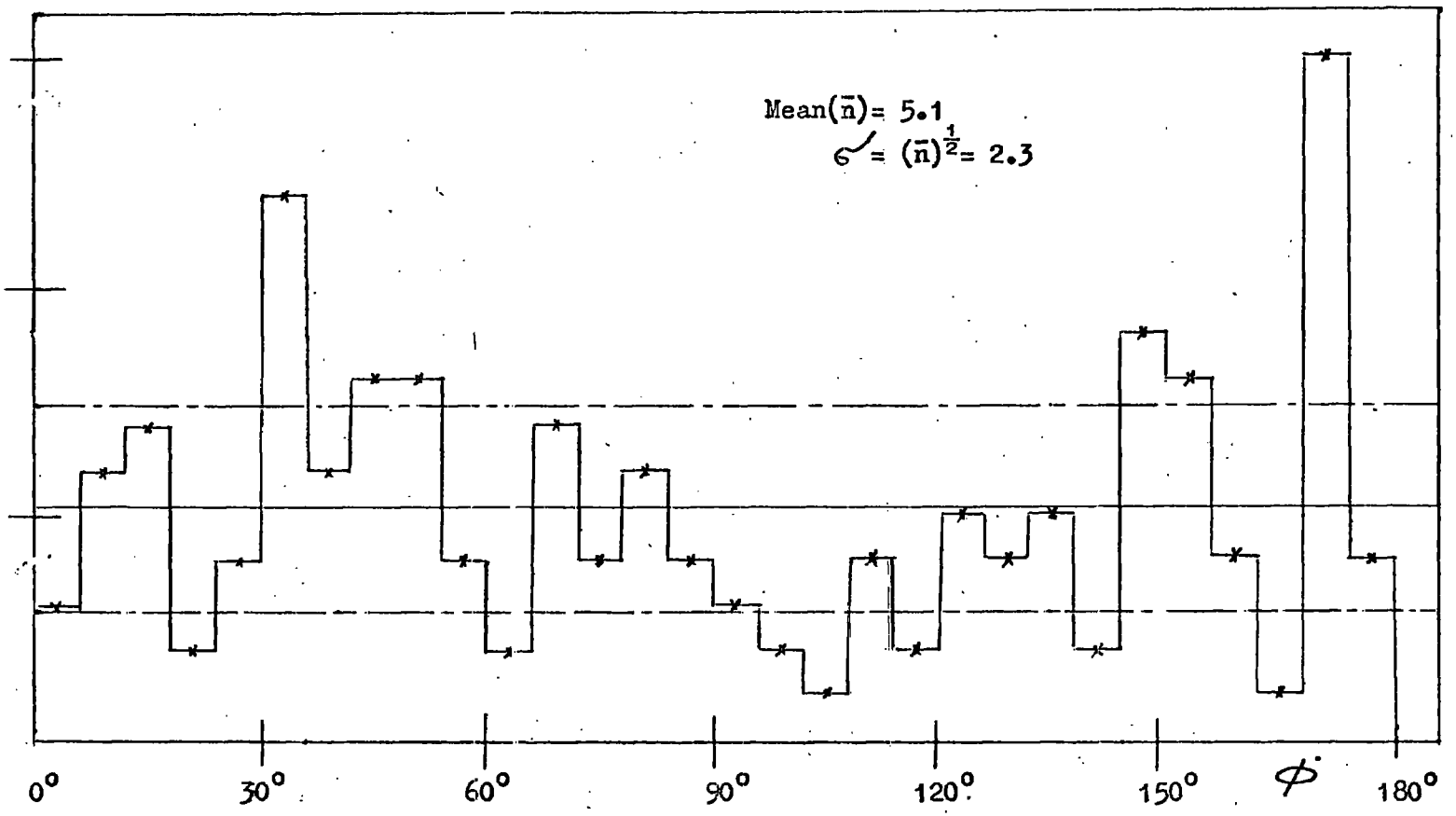

Fig. 4- Frequency function of galaxies against position angle in Hydra (Raw data).

To investigate further these seemingly significant peaks, we plot the histogram in the region of the peaks with a finer interval. The purpose of doing this is to see whether the surprisingly sharp rise at the peak is due to some excess at one position angle. The results for the two bigger peaks are given in figures 5 and 6 . They show that, in the case of Hydra there really does appear to be an excess at $171 - 2^{\circ}$.

In Virgo however, the position angles are spread quite evenly across the 6° bin . Since the accuracy of measurement is only about 5° this latter result is reasonable whereas the Hydra result seems quite suspicious.

A further test of the reality of these peaks is given by the spatial distribution of the galaxies concerned. It would for instance, be interesting if the galaxies were highly clustered.

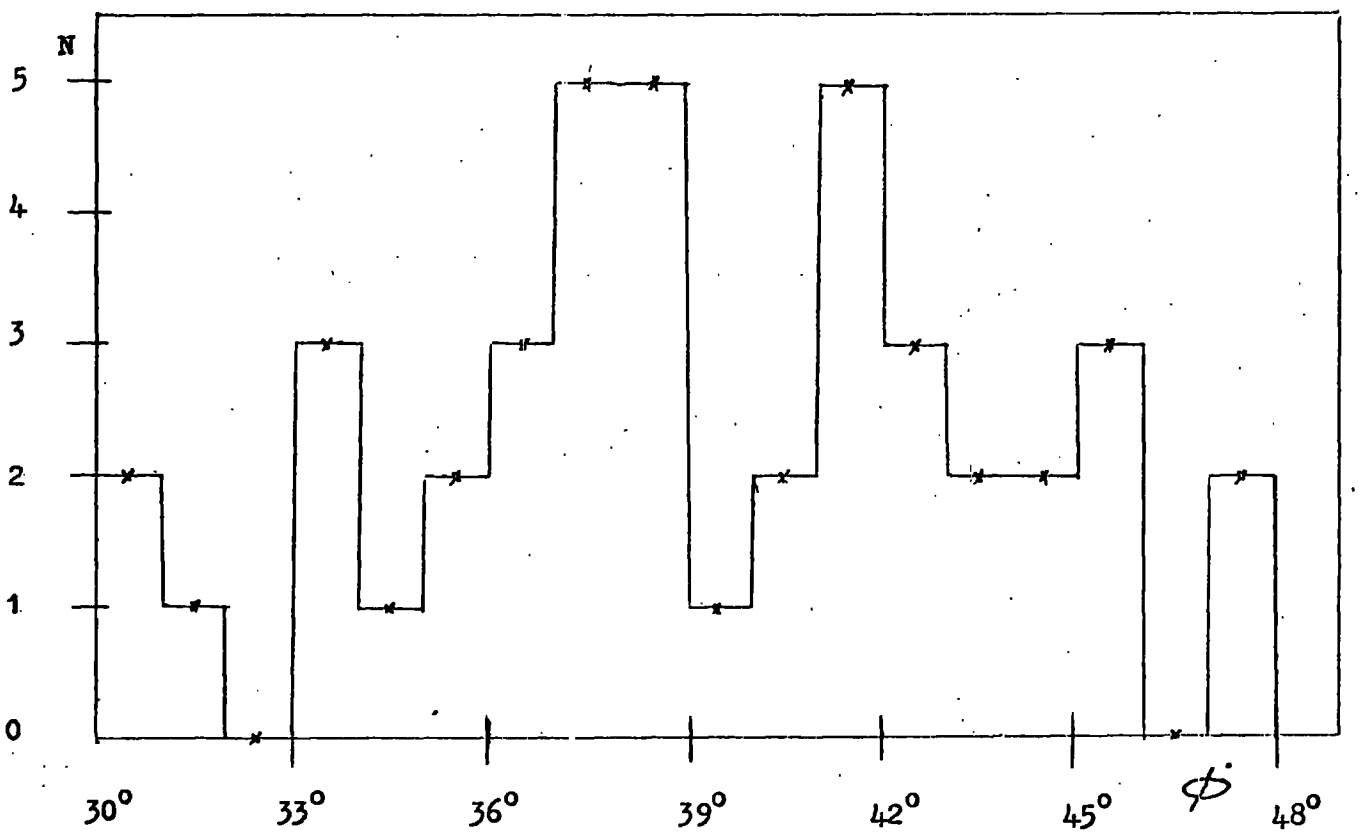

Fig. 5- Frequency function of galaxies against the position angle in Virgo (Raw data).

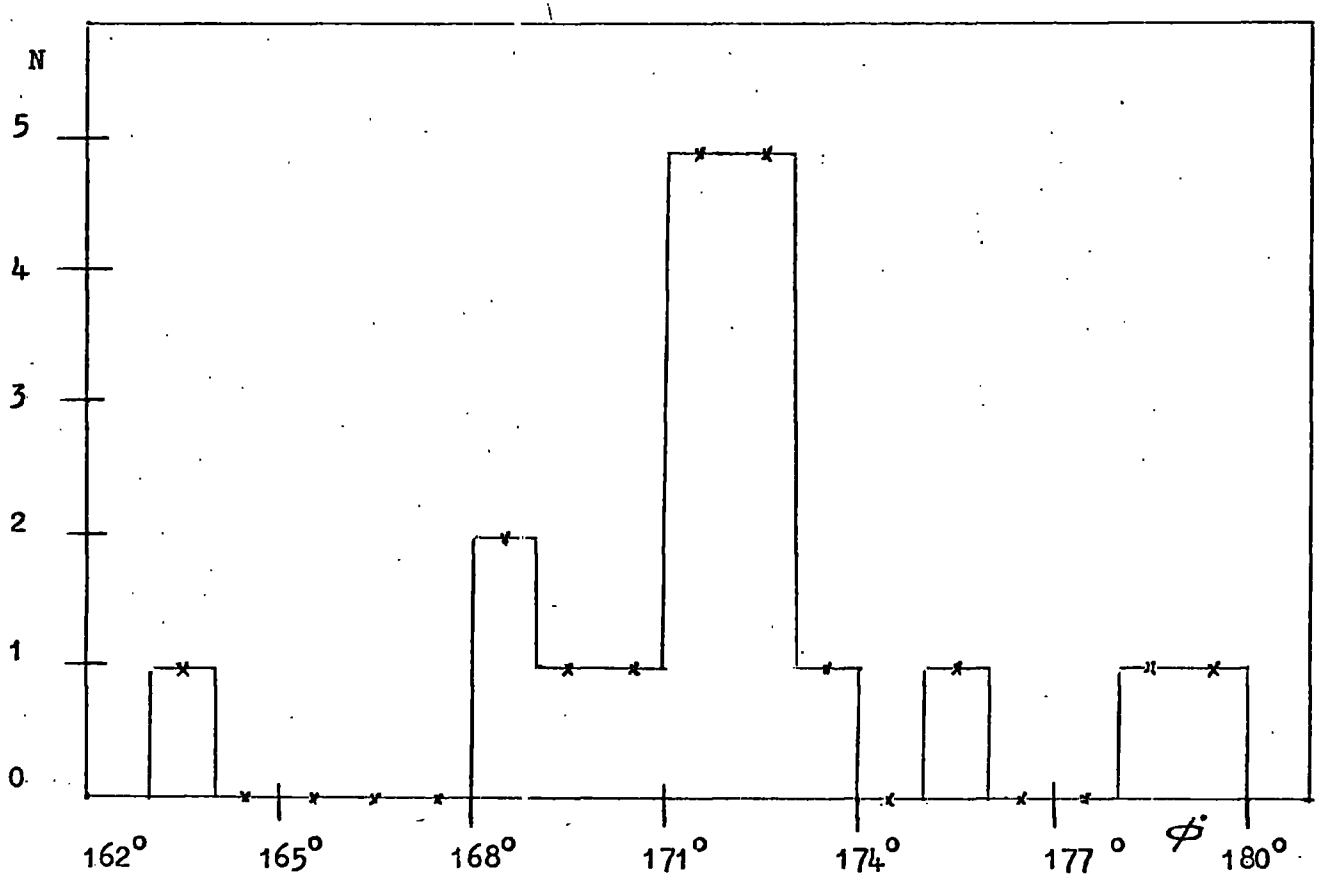

Fig. 6- Frequency function of galaxies agaist the position angle in Hydra (Raw data).

Table IV

Fractions of spiral galaxies in Virgo with position angles in the peak $30^\circ \leqslant \phi < 47^\circ$

PLATE NUMBER	FRACTIONS
1401	7/96 = 0.07
1405	8/86 = 0.09
1578	4/41 = 0.10
1023	3/62 = 0.05
1066	10/128 = 0.08
1600	10/131 = 0.08

Table V

Fractions of spiral galaxies in Hydra with position angles in the peak $162^\circ \leqslant \phi < 179^\circ$

PLATE NUMBER	FRACTIONS
28	8/82 = 0.10
922	2/87 = 0.02
233	4/74 = 0.05
649	1/78 = 0.01
1359	1/75 = 0.01
470	2/131= 0.02
1530	1/67 = 0.01

Table 3 and 4 show the fractions of spiral galaxies with position angles in the peaks mentioned above, for each plate in both areas.
Clearly there is little large - scale clustering on the Virgo area since the fractions vary by only $\pm$ 30 % .

On the Hydra data however, plate number 28 shows a marked excess of galaxies, though otherwise the distribution is quite even.
To examine this, and also to investigate the possible clustering of such galaxies on scales smaller than 6° the distribution of galaxies on individual plates was studied.

Figure 7 refers to such a distribution for the plate number 1600 in Virgo and figure 8, to plate number 28 in Hydra which we mentioned above. The positions are given by Brown to the nearest 0.5°only.

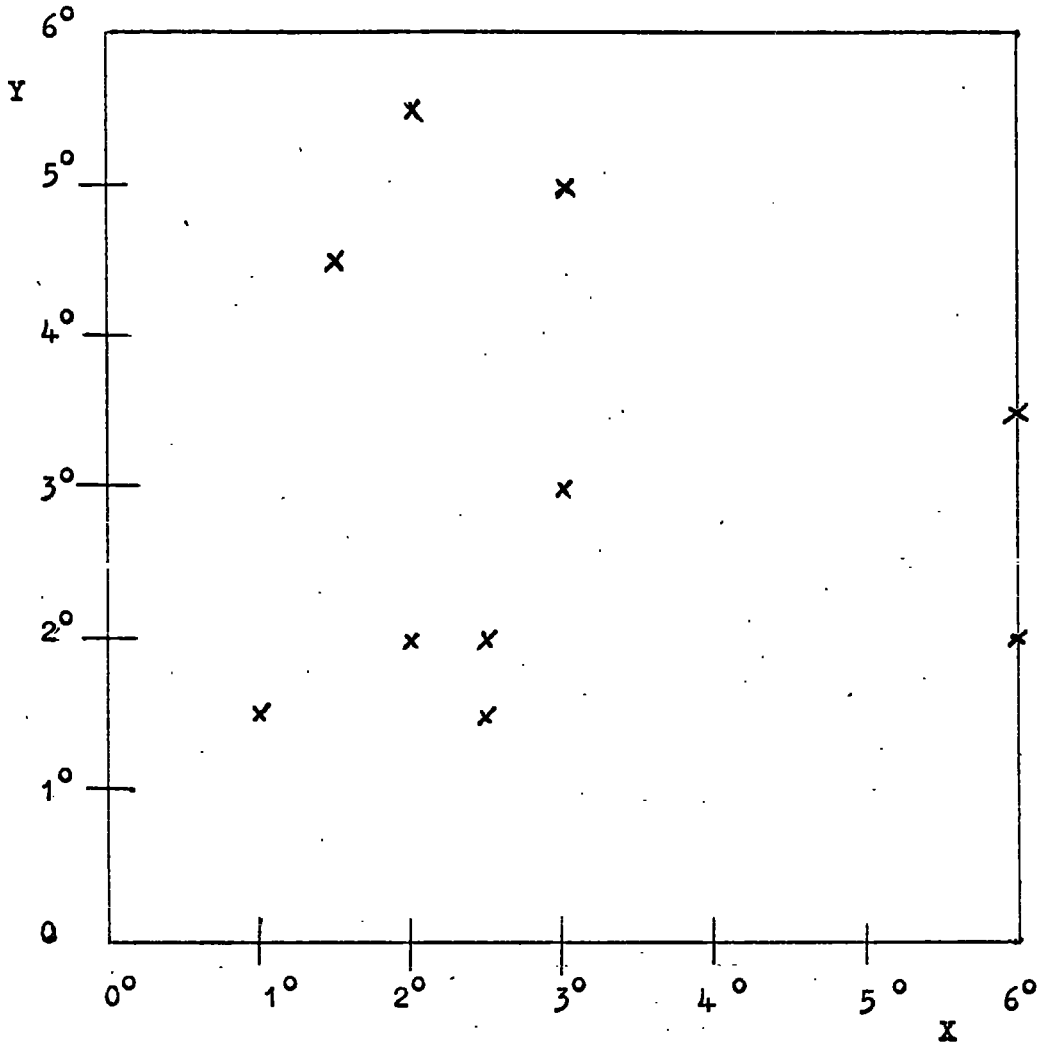

Fig. 7- Spatial distribution of galaxies on plate number 1600 in Virgo .

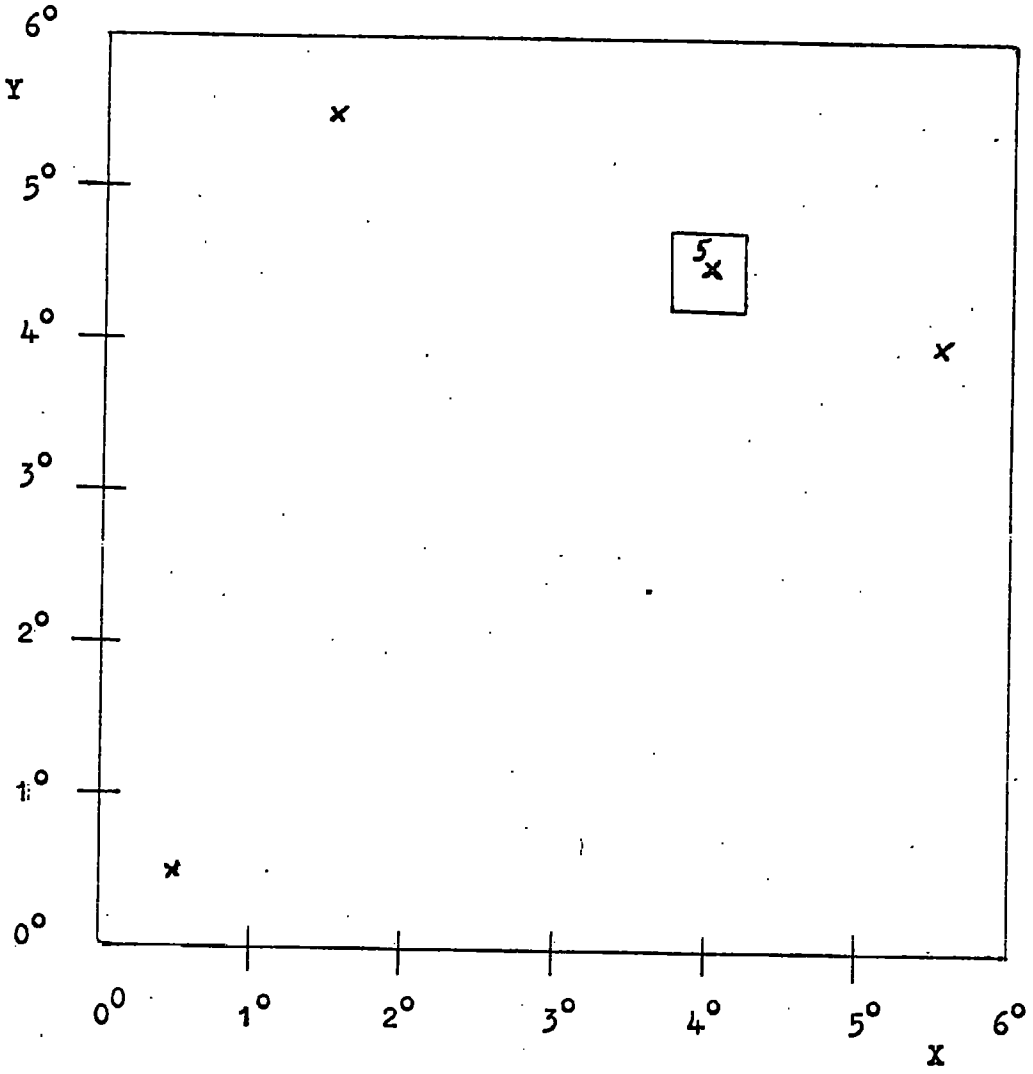

Fig. 8- Spatial distribution of galaxies on plate number 28 in Hydra .

We can measure the median of the observed separations between nearest neighbour of galaxies in figure 7 and 8, by hand and the results are as follows :

For plate number 1600 median of the observed separation $=1.15^{\circ}$

For plate number 28 median of the observed separation $=0.5^{\circ}$

We must note that in plate number 28 for Hydra, we have five within the same 0.5° X 0.5° square and having position angles between 169°-172°.

By using the following formula, we will be able to find expected median of the separations between nearest neighbour of galaxies in the figures 7 and 8 :

$$\exp(-\pi n/A\,\theta^{2}_{med.}) = \tfrac{1}{2}$$

where $\theta_{med.}$ is median angular separation between nearest neighbour galaxies, n is the total number of galaxies in each plate, and A is the area of the plates.

For plate number 1600 $\theta_{med.} = 0.9^{\circ}$

For plate number 28 $\theta_{med.} = 1.0^{\circ}$

Comparing the two values for the observed and expected medians, we find that they are quite close for Virgo, and therefore, the galaxy distribution in figure 7 is not significantly clustered. For the Hydra data however the situation is affected strongly by the 5 galaxies at the same co-ordinates.

The raw catalogue was checked and this seems to be a real effect which in itself is of some interest.

2.5 - Opik plots

Unlike axis ratios, little is known about possible selection effects that might operate when recording position angles; laboratory experiments like those of Holmberg(1946) would be most helpful. Opik once suggested(1970) that, one can combine the distributions of position angles and axial ratios to get a better picture of the distribution of angular momenta. Here we investigate this possibility by means of a polar diagram.

Opik (1970) suggested two-dimensional statistics in polar coordinates, P(position angle) and $R=(1-\text{Sin } i)^{\frac{1}{2}}$ (radius) with equal solid angles represented by equal areas in the two-dimensional projection.

According to figure 2 (chapter 1), i is the inclination and because of the finite thickness of a galaxy, we can substitute for Sin i, the apparent ratio of the axes (b/a), so that the polar coordinates become P and $R=(1-b/a)^{\frac{1}{2}}$.

Figure 9 represents such a polar histogram for a sample of galaxies in Virgo. Note that all axis ratios below 0.55 are included, but that the quantization of b/a seriously hampers the interpretation and use of the diagram.

It will be recalled that this sample shows a marked excess for $\phi \sim 36^{\circ}$ for $b/a < 0.3$. The plot reveals however, little evidence for a general clustering in this area on the two-dimensional plot.

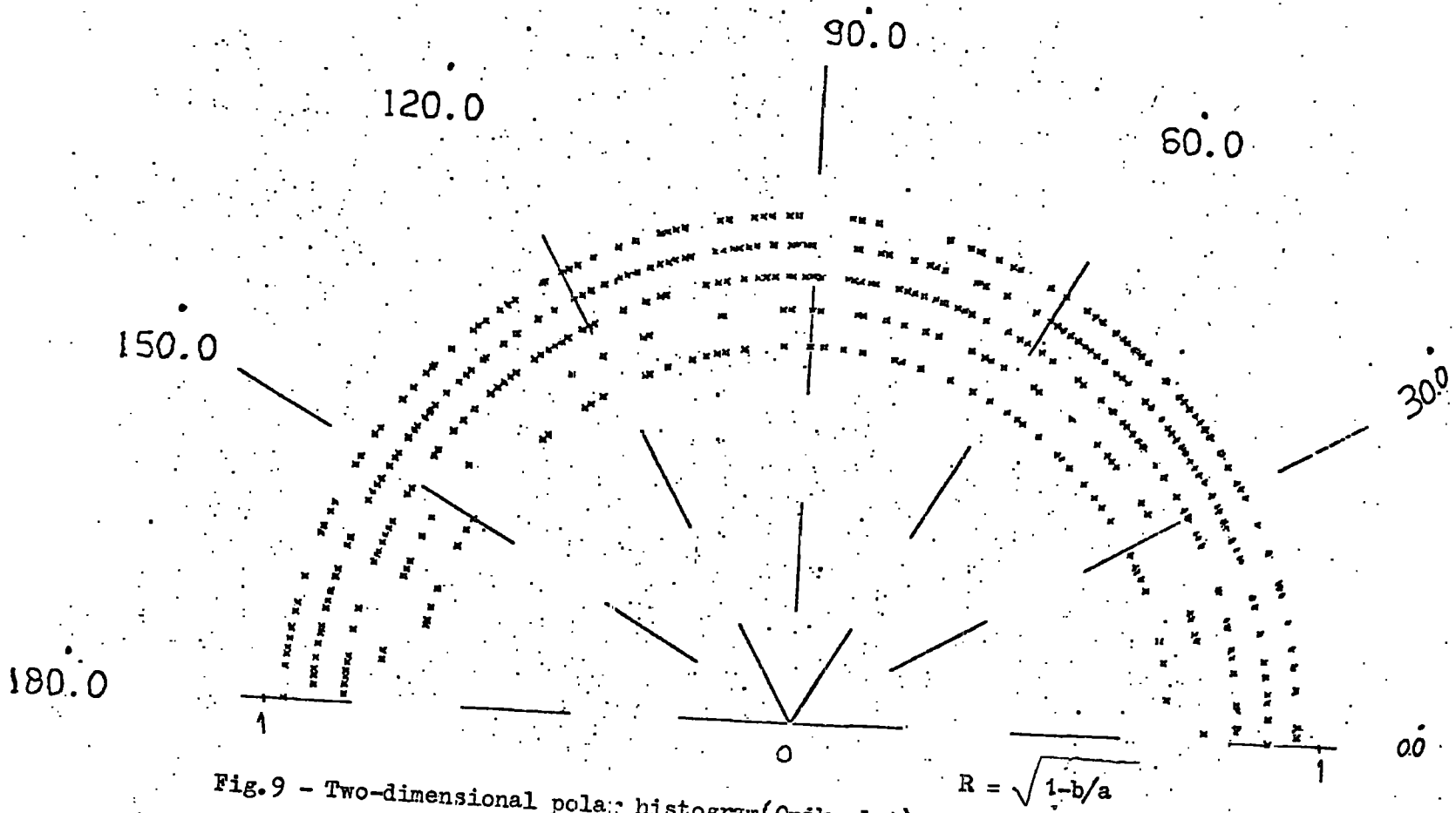

Fig.9 - Two-dimensional pola: histogram(Opik plot) of position angles and inclinations for Virgo .

2.6- Conclusion

Brown's investigation supports the view that there are significant departures from randomness in the distribution of position angles of galaxies in different regions of the sky. As we have seen, Brown moved galaxies to make the histogram smoother and found strong skew distributions of position angles. Our statistical tests (Chi-square and Autocorrelation) showed that the smoothness in Brown's histograms is not significant, though the smoothing has, if anything weakened the significance as determined by the χ^2 -test.

Among all of Brown's published histograms, there are two that show individual peaks significant at levels above 4σ. The total number of possible histograms is however quite large because of the various parameters Brown had at his disposal.

We estimate the total number of bins as follows :

6(regions) X6(forms)X5(sizes) = 180 , 180 X 30(bins) = 5400 bins

Therefore the probability of exceeding at 4σ once would be :

1 in 1600 / 5400

or

1 in 2.96

and for two peaks at 4σ the probability is :

1 in $(2.96)^2 = 8.8$, which is not very small.

A closer investigation of these peaks and the galaxies within them has not, however, given any further evidence that the excess is physical.

CHAPTER 3

ROE data

3.1- Description of ROE data

The data for this chapter are taken from a photograph of a field near the south galactic pole taken by the UK 48-inch Schmidt Telescope in Australia on nitrogen sensitized Kodak IIIaJ emulsion. Such photographs reach magnitudes B=23 in exposures of one hour (Corben, et al. 1974). In an area of 2(degree)^2 on this plate, 3054 galaxy positions, diameters, forms and orientations have been measured by Professor V.C.Reddish. In high southern galactic latitudes $\sim 10^5$ faint galaxies are measured on a single plate covering an area of sky 40(arcdegree)^2 (Dodd, et al.1975). Most galaxies are at distances of several thousand megaparsecs, and these galaxies probably have redshifts up to about $Z \sim 0.5$.

All measurements in the ROE data have been quantized. The positions are given to the nearest 254 μm (0.01 inch) and the axes to the nearest 10 μm.

The parameters of the photograph on which the measurements were made, have been given by Dodd, et al.(1975) and are reproduced in the table below :

Table V

Date :	1973 September 2-3
Plate number :	J - 149
Size :	14 in.X 14 in.
Emulsion :	Eastman Kodak IIIaJ, nitrogen sensitized.
Filter :	Schott GG 395
Exposure :	120 min.
Guiding :	Photoelectric

Plate centre (1973-5)	RA $02^h\ 42^{m}.0$, Dec. $-29^\circ\ 54'$
Sky brightness :	B = 22.1
Limiting magnitude :	$B \gtrsim 23$
Plate scale :	67 arcsec. mm^{-1}.

3.2- Frequency distribution of orientation angles

Of 3054 galaxies measured in the ROE data, 854 have measurable ellipticities(1-b/a) and hence position angles.

It is recognized that, insofar as these measurements (ROE) are concerned, several subjective effects, in particular selection effects of the type discussed by Opik (1969) and references therein, have most probably operated on the data. It is felt that investigations of this type, although subjective, are merited, especially in view of the deeper penetration in space of plates taken with the UK 48-inch Schmidt Telescope and the corresponding insight gained by approaches of this nature.

For the 854 galaxies, which have measurable position angles, the ROE data gives the angle to the nearest 1°. Figure 10 show the frequency distribution of position angles in 1° bins. It is immediately apparent that there are large peaks at $\phi = 0^\circ$ and $\phi = 90^\circ$ and that there are subsidiary peaks at multiples of 10° in ϕ . An explanation of this is that for the smaller or more nearly circular galaxies the error in measuring ϕ is much larger than 1° and there is a tendency to assign the value to the nearest multiple of 10°, this tendency being larger for galaxies with ϕ near to 0° and 90° . To reduce this effect we have, in figure 11 , replotted the same data regrouped into 10° bins centred on the multiples of 10°. The peak around 0° is no longer significant but that around 90° remains. It is also apparent that there are considerably more galaxies with $\phi < 90^\circ$ than with $\phi > 90^\circ$. That the observed distribution differs significantly from isotropy is borne out by

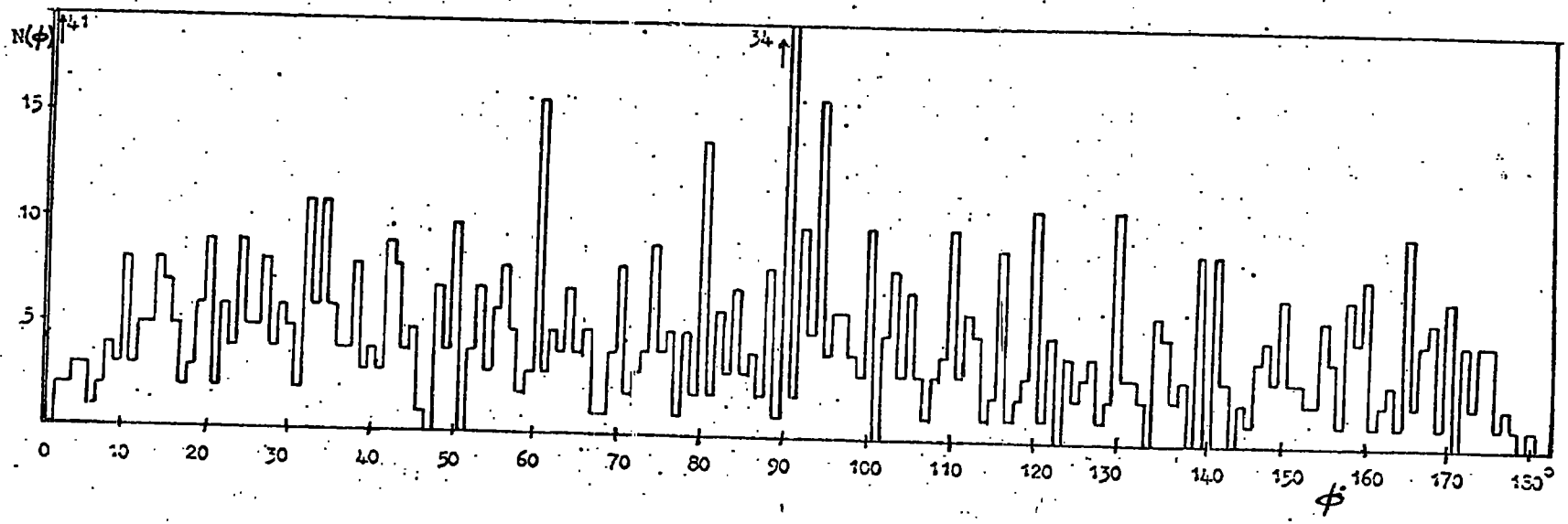

Fig. 10- Frequency distribution of position angles for 854 galaxies in 1° bin.

its χ^2 of 60.6 for 17 degrees of freedom ($P(\chi^2) < 10^{-4}$).

Although we can think of no measuring biasses that would favour $\phi < 90^\circ$ over $\phi > 90^\circ$ there is still the possibility that the peak around 90° is an artificial if there were a tendency to assign a ϕ of 90° to small galaxies or those having very small ellipticities. To investigate this, the distributions of sizes and axial ratios of the galaxies in the peak around 90° were compared with those for the complete sample of 854 galaxies. There was no excess of small or nearly circular galaxies in the 90° peak. As a final test the $N(\phi)$ distribution was found for the larger galaxies for which measuring error should be smaller . The dashed histogram in figure 11 is the distribution for 394 galaxies with $2a > 110'' m$. This is more uniform and the peak around 90°, although still present , is not statistically significant. The χ^2 against the hypothesis of isotropy is 14.1 ($P(\chi^2) = 0.8$).

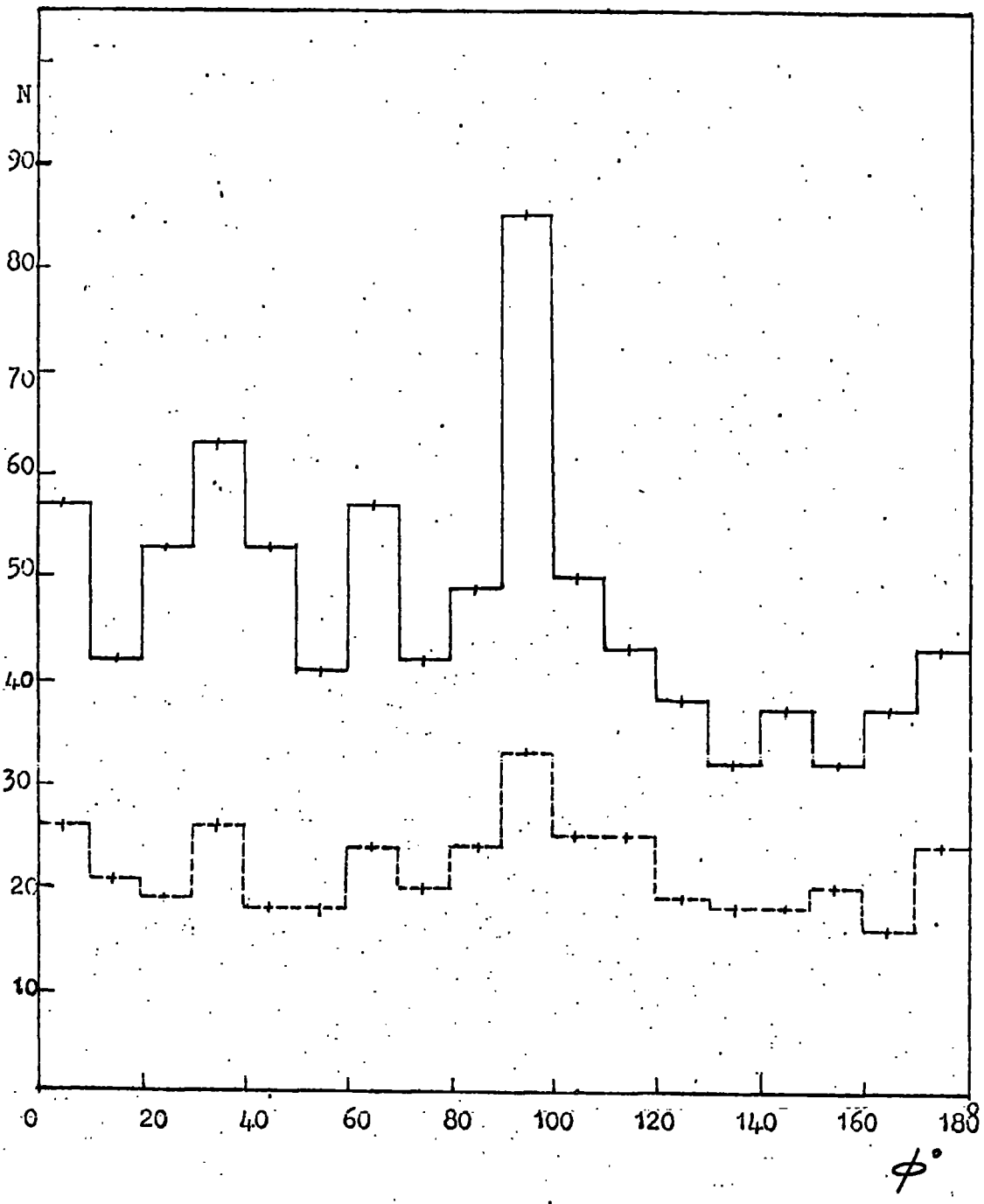

Fig. 11- Frequency distribution of position angles for total 854 galaxies (solid lines), and $2a \geqslant 110\mu m$ 394 galaxies (dashed lines).

3.3- Frequency distribution of difference between position angle of nearest neighbours

The material presented in this section is the observed histogram of the difference between orientation of nearest neighbour galaxies, on a UK 48-inch Schmidt Telescope plate.

The motivation for the search of distribution of orientations of neighbouring galaxies is that galaxies in any small region may have a preferred orientation, but that the preferred direction varies in a random way over scales larger than some coherence length or domain size (Howley, et al.1975). We can suppose that the angular momentum of internal rotation of galaxies must add to zero in small regions. Hence rotation axes would tend to be antiparallel and long axes parallel . Also we can say that if the coherence length were much smaller than the size of our regions the anisotropy would be averaged out.

The relative orientation $\Delta\phi$ of the pair is defined as the acute angle between position angles of nearest neighbours. We have counted in bins of 10° for ROE data, and they are plotted in the form of histogram in figure 12.

There is a difference between our histogram and histogram of Dodd, et al.(1975), because Dodd, et al. ignored any nearer galaxy with unknown position angle (Round galaxy) in measuring the difference between position angles of nearest neighbours, whereas in our plot of $\Delta\phi$, if the nearest neighbour to a galaxy with measured position angle is one with unknown position angle, we ignored both of them. Accordingly the total number of $\Delta\phi$ values is reduced from 854 to 181 .

In the following, the normal observational χ^2 parameter is used as a test of uniform frequency distribution , ie.,

$$\chi^2 = \sum_{i=1,n} \frac{(f_i^{obs} - f_i^{th})^2}{f_i^{th}}$$

where f_i^{obs} is the value from the observation and f_i^{th} is the mean number of galaxies per bin .

The observed distribution has χ^2=8.55 for 8 degrees of freedom. This has a probability $P(\chi^2)$ =0.4 and is this consistent with a uniform distribution. We note, that in any case that part of the excess for the $0^\circ$to 10° and 80° to 90° ranges of $\triangle\phi$ will be due to the artificial peaks at $\phi = 0^\circ$ and $\phi = 90^\circ$ that we noted in the $n(\phi)$ distribution .

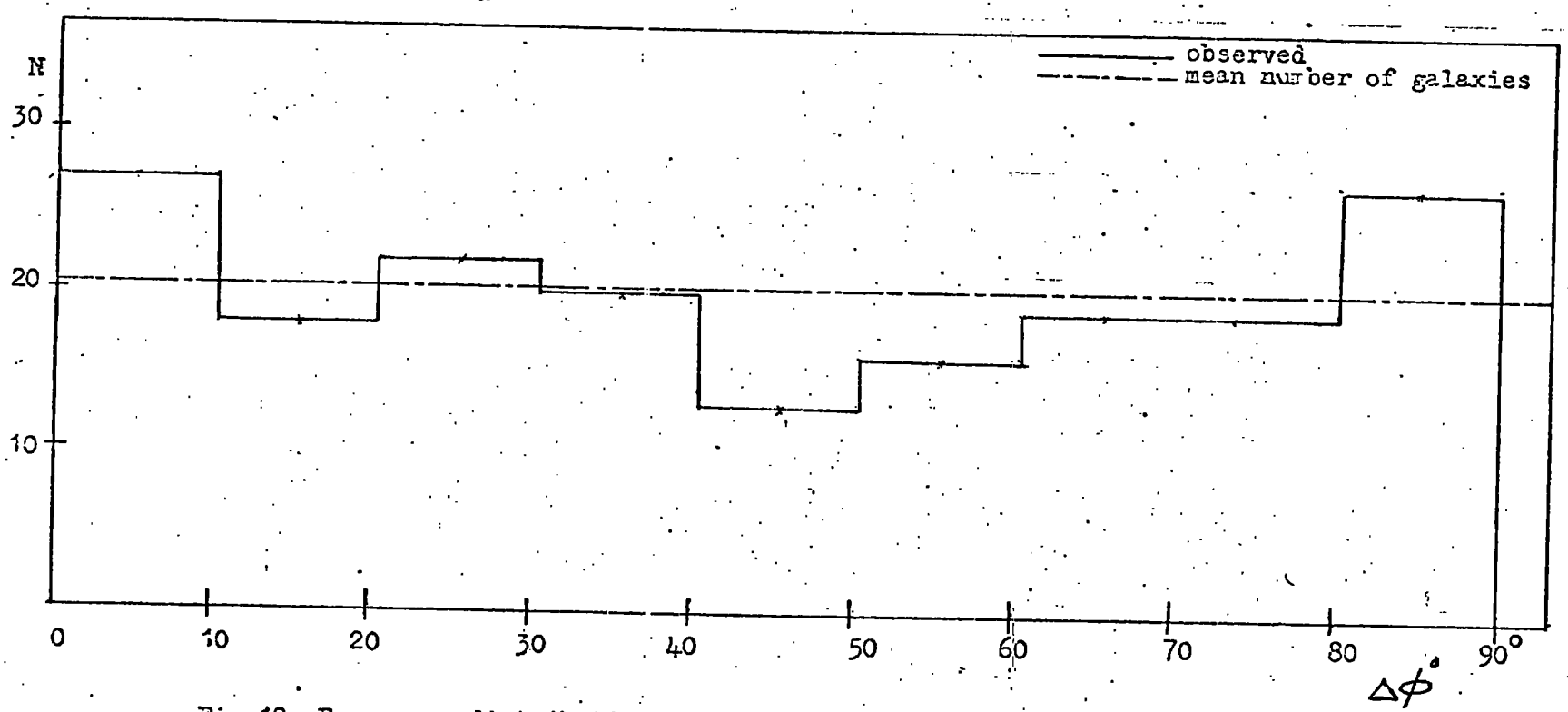

Fig. 12- Frequency distribution of difference between position angles of nearest neighbour galaxies.

3.4- The clustering of galaxies

a- General remarks

The spatial distribution of galaxies is a problem of great interest in cosmology and investigations are usually based on the following four main assumptions (Neyman and Scott, 1952) :

1- Galaxies occur only in clusters.

2- The number of galaxies varies from one cluster to another in a manner subject to a definite probabilistic law, the same for all clusters.

3- The distribution of galaxies within a cluster is random and is subject to a probabilistic law which also is the same for all clusters.

4- The distribution of cluster centres in space is random.

The tendency for galaxies to clustering has been known for some time. Most bright galaxies exist in systems of pairs, triplets or multiplets which are themselves usually subsystems of larger groups or clouds of galaxies (de Vaucouleurs, 1971).

In the published analysis of the distribution of galaxies in the ROE data Dodd, et al. (1975) state that the results are consistent with the hypothesis that all galaxies are contained in clusters containing from 2-6 members, and also they found evidence for small scale clustering.

Another recent analysis on the above data involves the angular covariance function for the distribution of the 3054 galaxies(Dodd, et al.1976). They found there is clustering of galaxies present with a scale length of 3000/~ m on the plate corresponding, at the typical distance of the galaxies, to a metric scale of 1 Mpc. Here we investigate these conclusions by comparing the observed frequency distribution of angular separation of nearest neighbour of galaxies on the same data, with that expected for a random distribution.

b- Observed and expected frequency distribution of angular separation of nearest neighbours

Figure 13 (solid lines) shows the observed angular separation of nearest neighbour galaxies counting mutual separations twice.

The expected distribution of nearest neighbour separations for a random distribution of galaxies on the plate is given by the dashed line.In calculating this, one has taken into account the quantization of positions, whereby the area of the plate is divided into 254 μm by 254 μm cells and the position quoted is the centre of the cell in which the galaxy falls. The probability distribution of recorded separations has been calculated as described in Appendix 1b and has been normalized to the total of 3054 galaxies. The recorded positions are plotted in 100 μm bins. One can see that the quantization effect is very important for small separations. The first three non-zero bins correspond to recorded separations of 0, 254 and 359 μm.

c- Comparison and interpretation

Figure 12 shows that the observed number of nearest neighbours with recorded separations of 254 and 359 μm are significantly greater than those predicted . Correspondingly there is a general deficiency of larger separations. This confirms that the galaxies are non-randomly distributed ie. that there is some clustering . One can combine the result of the nearest neighbour analysis with that of the covariance analysis, which gives a cluster diameter of $\sim$3000 μm to get a rough estimate of the number of galaxies in a cluster . Let us assume that the small separations are recorded almost entirely by galaxies in clusters. To account for the excess of small separations the mean density of galaxies in the clusters must be greater than the overall mean density of galaxies on the plate.

In particular the observed frequency of 254 μm and 359 μm separations will be reproduced if the density of galaxies in a cluster is 0.06 per 254 X 254 μm^2 cell compared with 0.03393 for the overall mean density. Multiplying the former density by the area of a 3000 μm diameter cluster gives an estimate of 6.5 galaxies per cluster.

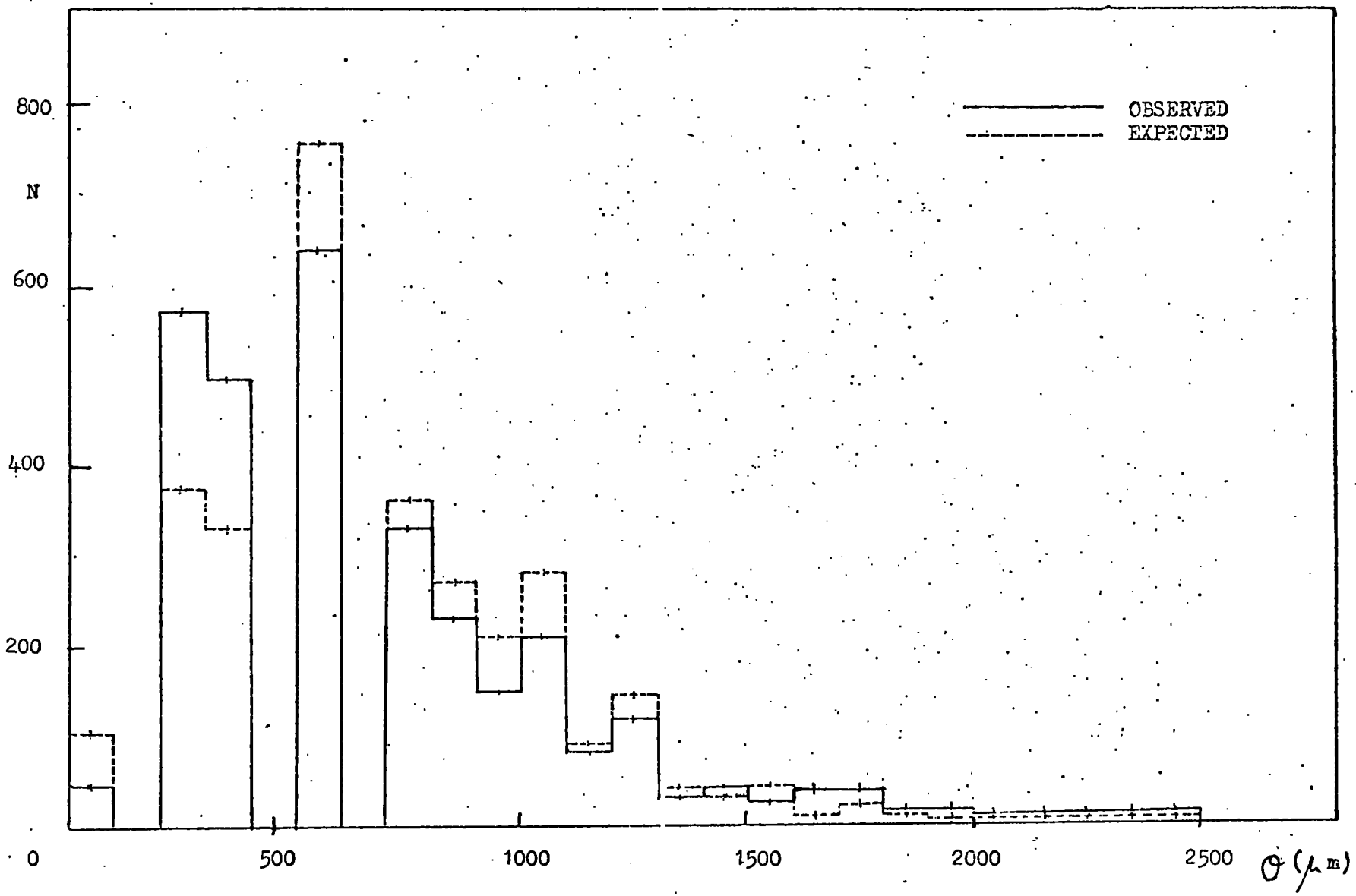

Fig. 13- Comparison of the observed frequency distribution of angular separation of nearest neighbours with that predicted for a random distribution of galaxies on the sky.

3.5 - Distribution of axial ratios

a- General remarks

Assuming a random distribution of the three dimensional orientation of galaxies, it is possible from the distribution of axial ratios to find the fraction of spiral and elliptical galaxies . This is of interest since we have little knowledge of such a fraction at the epochs corresponding to the data observed on deep plates.

The galaxy classification systems which are conventionally used are based on the two-dimensional images of galaxies and therefore do not necessarily characterize the true three-dimensional form of the object. There is no easy way of constructing a three-dimensional model from the two-dimensional plate, but by using dynamical arguments or statistics it is possible to obtain information on true forms of galaxies. For instance, an E0 galaxy might be spherical or it might be a very eccentric ellipsoid viewed face-on . Eventually, it is hoped that exceedingly high-precision photometry might be able to distinguish between these possibilities, but so far the distribution of orientation of elliptical galaxies has only been attacked statistically.

Model for true distribution of axial ratios

The frequency function of true axial ratio (r_0=B/a) of spheroidal galaxies can be derived easily from the observed frequency function of apparent axial ratios (r = b/a) under the assumption of random orientation of the spin axes. This problem has been often treated , mainly with respect to elliptical, lenticular and spiral galaxies and most recent by Sandage et al.(1970) from statistics of the BGC data (de Vaucouleurs, 1959). In this section we reanalyze this problem on the basis of the expected frequency function of axis ratios with semi-major axis between 100 $\sim$ m and 400 $\sim$m in the ROE data.

According to shapes given by Sandage et al.(1970) , the frequency distribution of apparent axial ratios for spirals and S0 types is centred at about r=0.25,and has small dispersion . A single Gaussian with r_0=0.25 and σ=0.06 is used for both the S0 and SB0 and the Sa, Sb,and Sc groups. The result that elliptical galaxies may not be uniformly distributed in r, but may have a peak near r=0.6 is of some cosmogonic interest . A single Gaussian with r_0=0.65 and σ=0.18 is used for elliptical galaxies.

The relative abundances of different types of galaxies

When galaxies were first catalogued,it was thought that the spirals were far more numerous than any of the others, though some investigators believe that there are as many ellipticals as there are spirals. Hubble(1936) obtained the accompanying table (table VI) of relative abundances of different types of galaxies. We must, however realize that in this sort of frequency analysis,selection and sampling play a very important role since we classify into groups only those galaxies whose structure can be clearly resolved, and these are generally the galaxies with large apparent diameters.

Table VI

Relative frequency of galactic types

Type	Frequency(per cent)
E0 - E7	17
Sa, SBa	19
Sb, SBb	25
Sc, SBc	36
Irregular	2.5

A survey of photographic plates of extragalactic objects shows that the greatest number of images is very small objects whose structures can not be discerned with sufficient accuracy to allow classification. Hubble(1926) in his analysis used only the very brightest galaxies listed in the catalogue of Shapley and Ames, so that no question could arise as to the classification of these galaxies. We must therefore expect to find strong departure from these abundances in local samplings, and, indeed, we know that in many clusters of galaxies the number of ellipticals is greater than that of spirals. Within our own Local group of galaxies consisting of 17 individual members, there are probably nine ellipticals.

According to deVaucouleurs (1963), for $m_{pg} < 12.7$ the proportion of galaxies in each class is approximately as follows:

E	13 %
S0	21.5%
S, SB	61 %
Irr.	2.5 %
Uncertain	2 %

If we add S0, S, and SB together and ignore the Other classes we would have :

Ellipticals	14 %
Spirals	86 %

Van den Berg (1975) obtained another frequency of classification as table VII .

Table VII

Relative frequency of classification of galaxies

Type	Percentage
E+S0	22.9
Sa	7.7
Sb	27.5
Sc	27.3
Irr.	2.1
Others	12.5

He does not separate the E and S0 galaxies. In the Reference Catalogue of Bright Galaxies (de Vaucouleurs, et al. 1964) the total numbers of E and S0 galaxies with measured redshifts are 177 and 174 respectively. In the above table we therefore take it that these should be 11.5 % for E only.

Adding S0 into Sa+Sb+Sc and omitting the Irr. and ' Others' we obtain :

Ellipticals	15 %
Spirals	85 %

which is close to that of deVaucouleurs.

Remarks on selection effects and their corrections

The discovering of galaxies is severely limited by observational selection of surface brightness and apparent diameters. Galaxies having an average surface luminosity less than μ_B=27 mag.(arcsec^{-2}) are not optically detectable by present techniques. Galaxies having an apparent diameter less than $\sim 1''$ are not readily distinguishable from stars with current instruments (deVaucouleurs,1974). It is probably not by accident that the average surface brightness of the so-called 'normal'galaxies is only slightly above that of the night sky(de Vaucouleurs, 1957).

Further selection effects arise in the formation of catalogues.

As we know, the selection effects are different for spirals and ellipticals. Reinhardt(1972) has given the following formula for correction of selection effects known to operate on axial ratio measurements.

1- Correction for first Holmberg effect :

$$(b/a)_{corrected} = (b/a)^{0.745}_{apparent} \qquad \text{For ellipticals}$$

$$(b/a)_{corrected} = (b/a)^{0.812}_{apparent} \qquad \text{For spirals}$$

In ROE data we used the average powers of above formula, because we are not able to distinguish between spirals and ellipticals, that is :

$$(b/a)_{corrected} = (b/a)^{0.778}_{apparent}$$

2- Corrections for second Holmberg effect and Opik effect :

$$D(r)_{apparent} = D(I)\, r^{-0.169}_{corrected} \qquad \text{For Spirals}$$

$$D(r)_{apparent} = D(I)\, r^{-0.296}_{corrected} \qquad \text{For Ellipticals}$$

$r = (b/a)$

where D(r) is the maximum diameter (apparent) and D(I) is a corrected " face on " maximum diameter.

b- Observed and expected frequency distribution of axis ratios

Figure 14 shows the histogram of axial ratios for 3054 galaxies. In this histogram we see 2221 galaxies with b/a = 1 . This is mainly because of large quantization effects in the measurements.

The smallest non-stellar images measured have diameters 2a = 50μm (3.3 arc sec) . Above this, values of 2a and 2b are given to the nearest 10μm. The lower limit to 2b is also 50μm. Thus all galaxies with 2a = 50μm will have a recorded axial ratio b/a = 1 while those with 2a = 60μm will be divided between b/a =1 and b/a =0.83 and so on. The effect of the seeing disc of 30μm(2 arc sec)diameter also has to be considered. It can be approximately accounted for by subtracting 30μm from the measured values of 2a and 2b . It is apparent that for the smaller galaxies which dominate the data the quantization effects and the correction for seeing are of overwhelming importance and it is doubtful whether any useful information on the intrinsic forms of galaxies can be obtained from the overall distribution of axial ratios. Hence we restrict the range of major axis in the observed histogram of axial ratios to those between $100\mu m \leqslant 2a \leqslant 400\mu m$. Figure 15 shows the frequency distribution of axial ratios for the 779 galaxies with major axis in the above range. As the correction for seeing is of less importance for these galaxies we initially ignore it. It is considered at the end of this section.

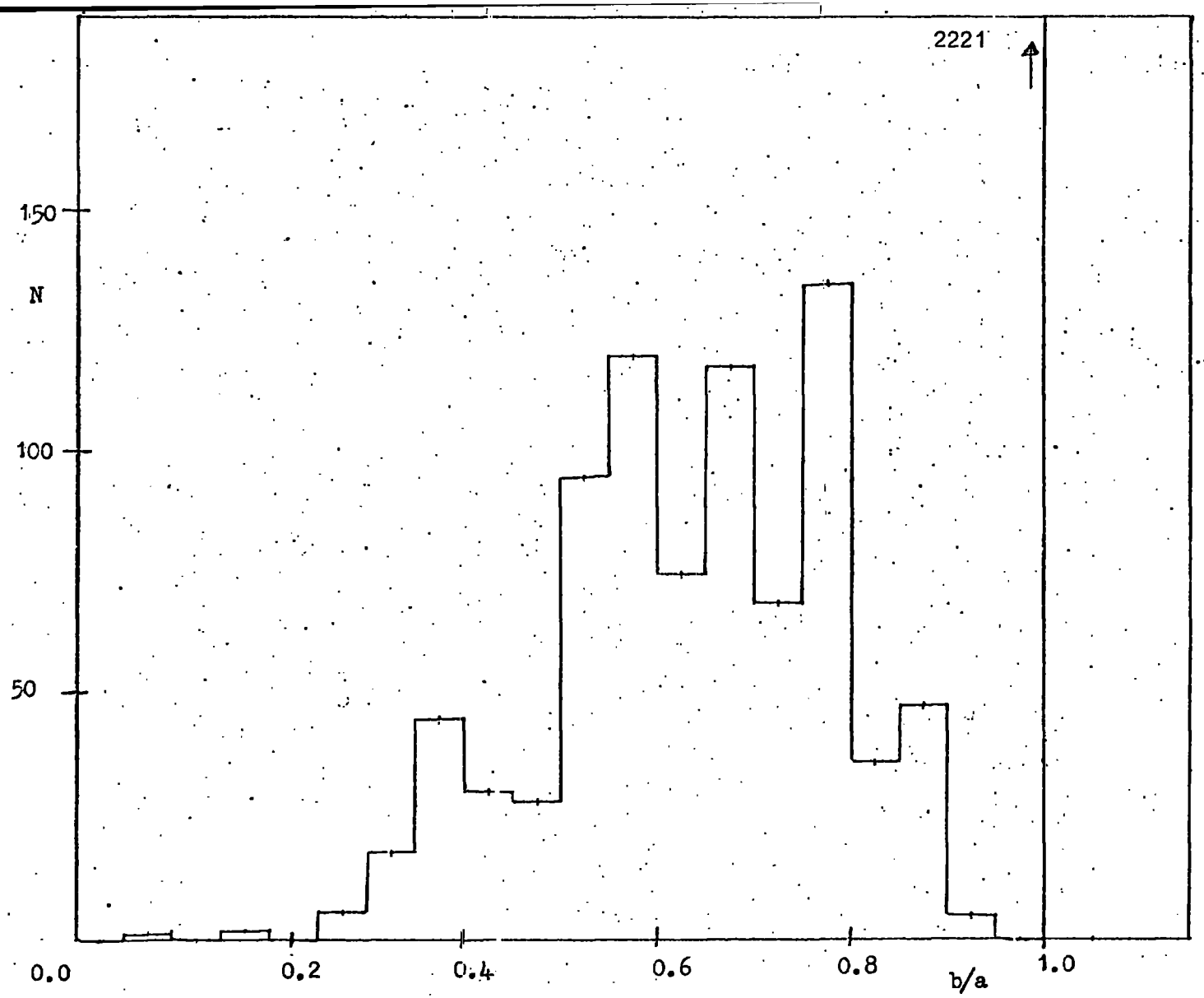

Fig. 14- The observed frequency distribution of axial ratios for the 3054 galaxies.

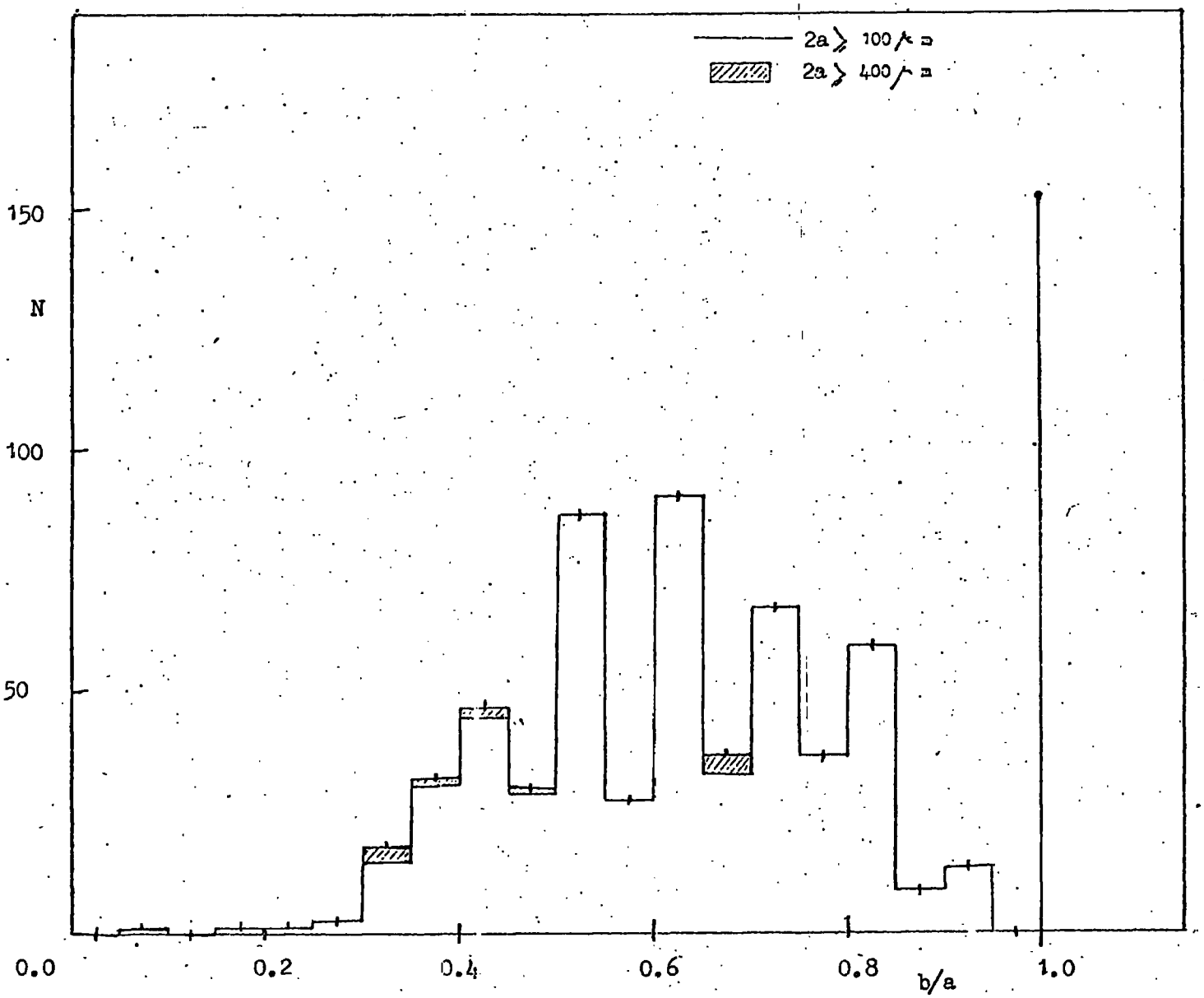

Fig. 15- The observed frequency distribution of axial ratios of galaxies with angular diameter equal or greater than 100 μ m.

For interpreting of the observed histogram, we plot first of all the expected frequency function (i.e. differential distribution) of axial ratios of galaxies, without using corrections for the Holmberg and Opik effects (chapter one), that is ;

$$f(r) = r\left[(r^2-r_o^2)(1-r_o^2)\right]^{-\frac{1}{2}}$$

where $r_o=B/a$ is true axis ratio (for further details about frequency function and frequency distribution equations, see appendix 2). The quantization has been allowed for.

Figure 16 shows this expected distribution of axial ratios for four different values of r_o . In these histograms, the effects of quantization can be clearly seen.

For each major axis value the predicted number of galaxies with $2b \leqslant 50\mu m$ have been summed . This gives a peak in the distribution at $b/a = 0.5$ for those galaxies with $2a = 100\mu m$. Since galaxies of this size give the largest single contribution to the total there is a peak at $b/a = 0.5$ in the overall distributions that have $r_o=B/a < 0.5$.

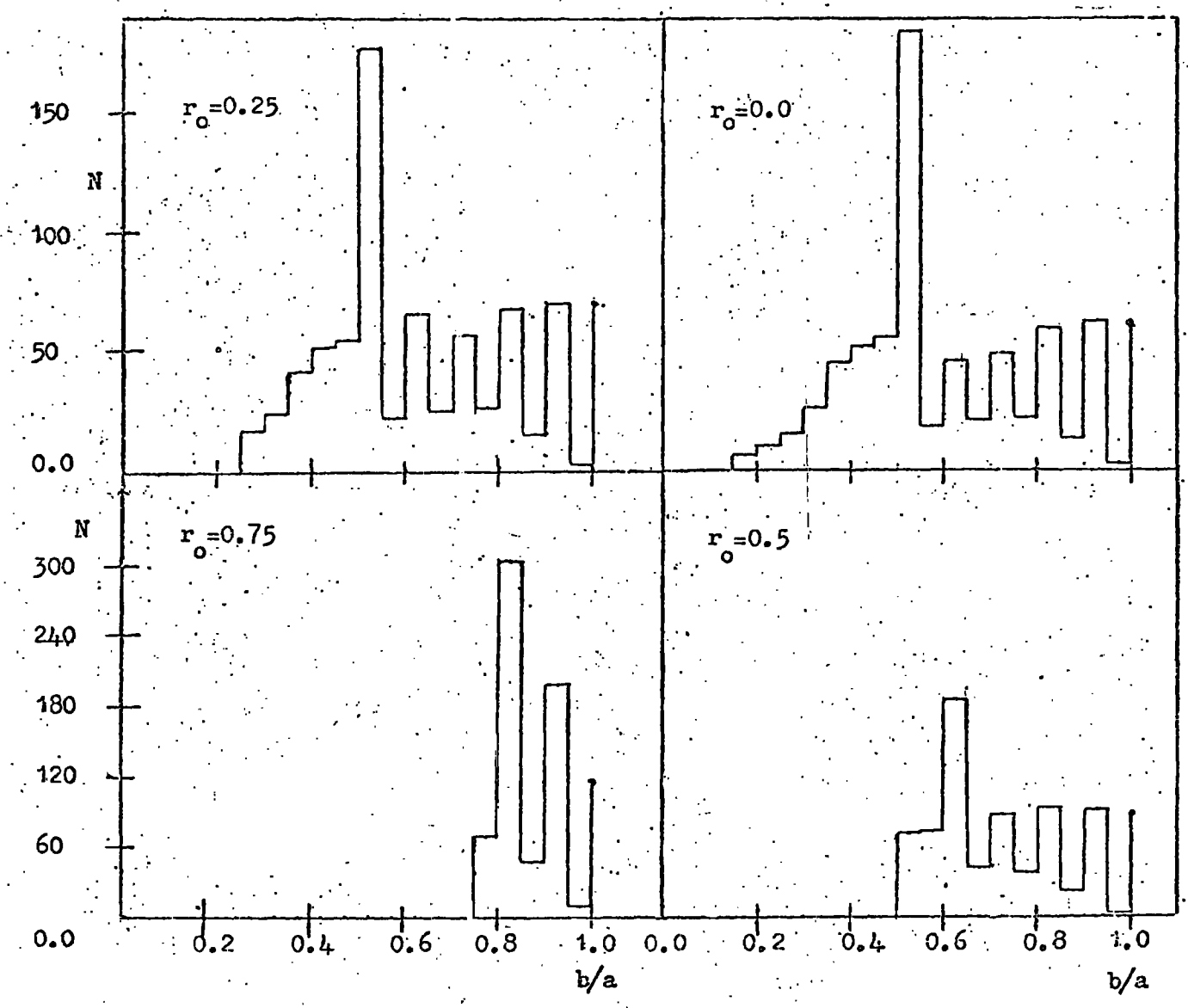

Fig. 16- The expected frequency distribution of axial ratios of galaxies for four different values of true axial ratio.

Now to account for the selection effect discussed in chapter one, we must multiply the frequency function by a selection function $S(r)$. For the second Holmberg effect and the Opik effect, we are effectively considering different volumes for different axial ratios with the same limiting angular diameter. Assuming a constant space density the number of galaxies entering the catalogue will be proportional to the respective volumes, ie., to $\left[D(r)/D(1) \right]^3$, therefore this gives us with the Holmberg correction (Reinhardt, 1972) ;

$$S(r) = (r^{-0.336})^3 \simeq r^{-1.01}$$

or

$$S(r) \simeq r^{-1}$$

hence from above :

$$f(r) = \left[(r^2 - r_o^2)(1 - r_o^2) \right]^{-\frac{1}{2}} \text{ X const.}$$

If we integrate between r and r_o , we find the normalized distribution function as follows :

$$F(r) = \int_{r_o}^{r} \left[(r^2 - r_o^2)(1 - r_o^2) \right]^{-\frac{1}{2}} \text{ X const.} \cdot dr$$

$$F(r) = \text{Log } (r + (r^2 - r_o^2)^{\frac{1}{2}} / r_o) \; / \; \text{Log } (1 + (1 - r_o^2)^{\frac{1}{2}} / r_o)$$

In figure 17, we have plotted the expected distribution function of axial ratios allowing for the above selection effects, for the four different values of r_o . In these histograms we see the main effect of the corrections is to shift the numbers to smaller b/a.

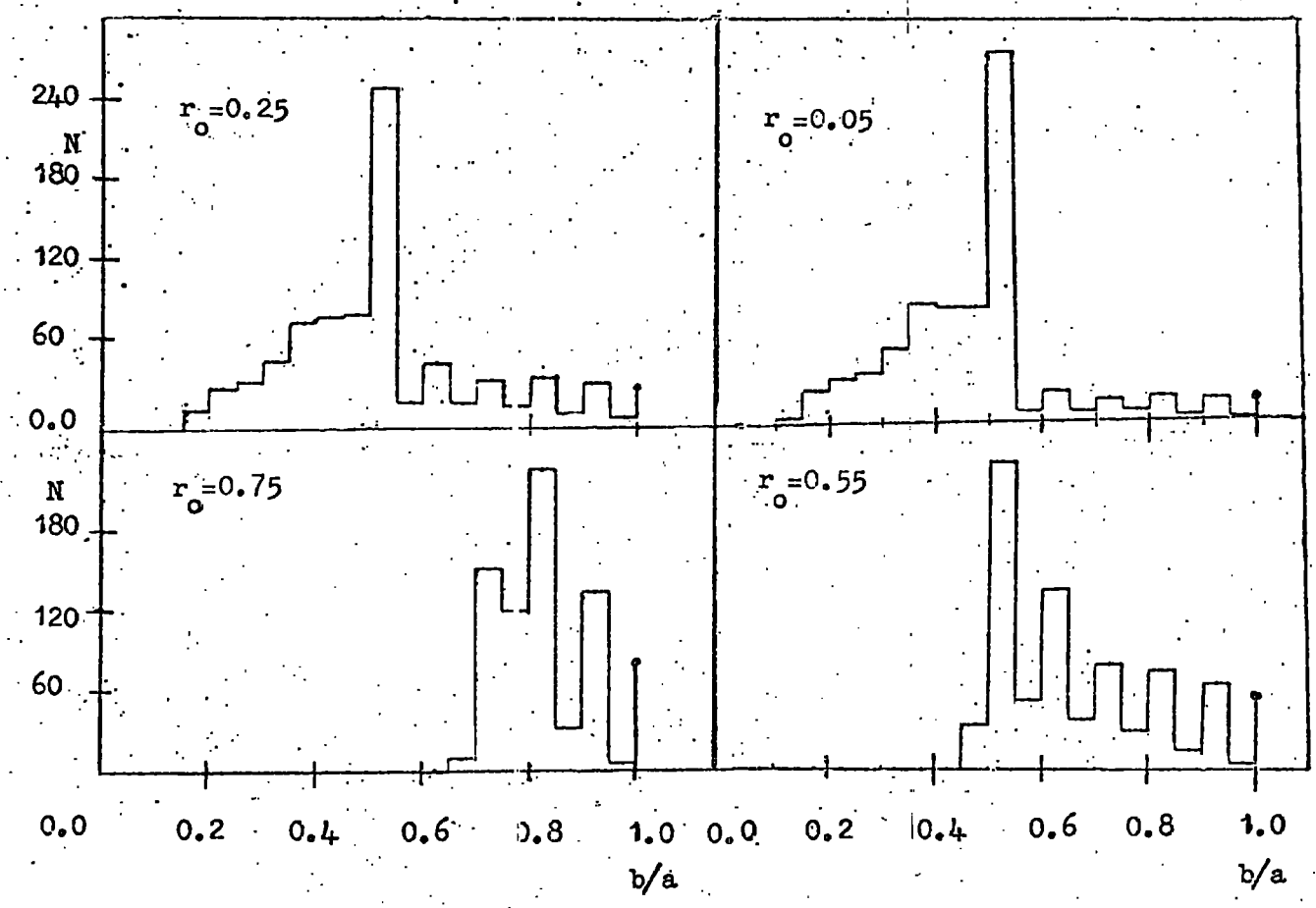

Fig. 17- The expected distribution function of axial ratios allowing for the selection effects, for the four different values of true axial ratios.

Fraction of elliptical and spiral galaxies in the ROE data

By weighting the previous histograms according to distribution of true axial ratios for elliptical and spiral galaxies given by Sandage et al.(1970), we plot expected histograms for spirals and ellipticals separately. Figure 18 shows the observed frequency distribution ($100\mu m \leqslant a \leqslant 400\mu m$)together with the expected frequency distribution of ellipticals and spirals . According to figure 18, if we compare observed frequency distribution of axial ratios with the expected frequency distribution of spirals and ellipticals, we still find that there are too many galaxies with axial ratios of one. This is matched by a deficiency in the range $0.8 \leqslant r=b/a \leqslant 1$ which suggests that there is a tendency for nearly circular images to be given an axial ratio of one. There is also the possibility that there is a residual contamination of the data by stars which will all have r =1. We therefore ignore the galaxies with r =1 in comparing predicted and observed distributions.

We performed a chi-square test on the observed and expected frequency functions as follows .

If we suppose that G is the fraction of galaxies which are spiral and (1-G) is the fraction of galaxies which are elliptical, the expected frequency function for spirals and ellipticals together is :

$$f^{exp.} = G \cdot f_S(r) + (1-G) \cdot f_E(r)$$

where $f_S(r)$ is the expected number of spiral galaxies in each bin of r and $f_E(r)$ is the same for ellipticals. Therefore, we have:

$$\chi^2 = \sum (f^{obs.} - f^{exp.})^2 / f^{exp.}$$

and we minimise χ^2 to find the best fit value of G.

We find a minimum value for χ^2 of 126.84 for G=0.30 . This value of χ^2 with 19 degrees of freedom is much too large for the fit to have

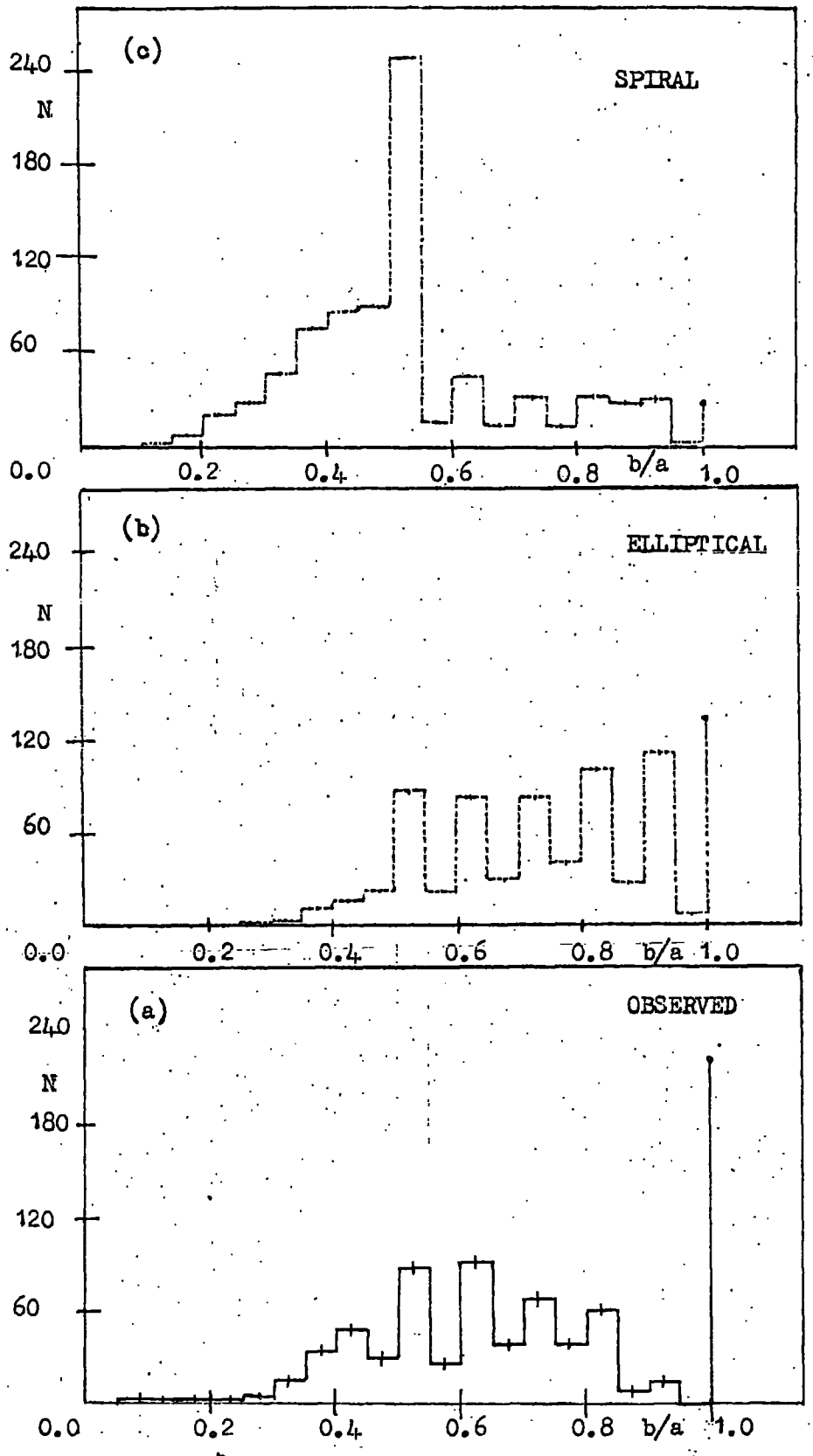

Fig. 18- (a) The observed frequency distribution of axial ratios. (b) The expected frequency distribution of axial ratios for ellipticals. (c) The expected frequency distribution of axial ratios for spirals.

any meaning . This is obviously a poor fit because the predicted frequency function of spiral galaxies (in figure 18) is quite different from the observed function, mainly because of the large peak at $r = 0.5$. This peak is largely due to the galaxies with $2a = 100\mu m$ for which the minimum $b/a = 0.5$. The seeing disc correction of $30\mu m$ is still important for galaxies of this diameter. As a final correction we take this into account. Following Dodd et al. (1975) $30\mu m$ is subtracted from the major and minor diameters of all galaxies. The observed frequency distribution of corrected b/a is shown in figure 19 for the 339 galaxies having corrected major diameters between $10\mu m$ and $40\mu m$. Again an attempt was made to find the best value of G, the fraction of spiral galaxies in the sample, using the predicted b/a distribution for spirals and ellipticals of figure 18 . It is obvious that no value of G will give a fit to the observed distribution for $r > 0.9$. As it seems likely that most galaxies with $0.9 < r < 1$ have been recorded as $r = 1$ we fit only to the observations for $r < 0.85$. The best fit value of G is 0.83 and the predicted distribution for this, normalized to the total observed number with $r < 0.85$, is also shown in figure 19 . It is interesting that with this normalisation the predicted total for $r \geq 0.85$ is 41 while the observed total is 43. Thus the observed excess at $r = 1$ can be accounted for by the deficit of nearly circular galaxies and no real excess of $r = 1$ galaxies is indicated .

The best fit of predicted to observed numbers has $\chi^2 = 48.5$ for 15 degrees of freedom. This is better than the previous case but the large χ^2 still casts doubt on the value of G obtained. The worst discrepancy is for $0.5 < r < 0.6$.

It is possible that in practice the lower limit on the measured values of 2b is not so clear cut as has been assumed in deriving the predicted curves . This would widen the peak in the predicted distribution .

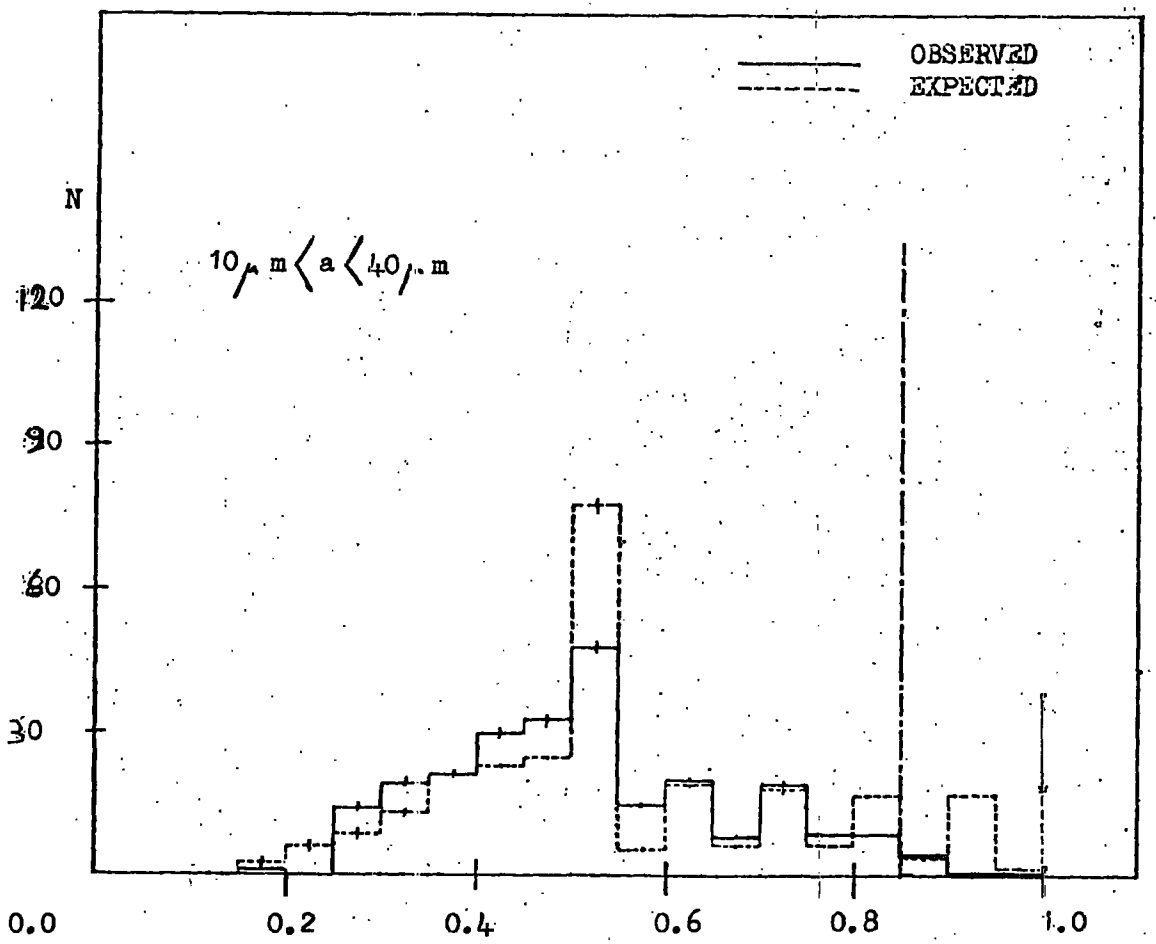

Fig. 19- Frequency distribution of axial ratios after subtracting 30 μm from 2a and 2b .

——— Observed distribution for counted 2a between 100 μm and 400 μm.

----- Predicted distribution, normalised to the total observed number with b/a < 0.85 for the optimum proportions of spirals and ellipticals (Viz, 83% spirals, 17% ellipticals).

We conclude that the distribution of observed axial ratios for galaxies with corrected major diameters $\geq 100\mu$m is consistent with that predicted assuming the normal mixture of spirals and ellipticals. A stronger statement can not be made because of the necessity of invoking plausible but unsubstantiated biasses in the measurements to account for discrepancies.

3.6- Conclusions

The results of the present investigation are brought together in the following summary. The main conclusions relate to four points : (a) the distribution of position angles, (b) frequency distribution of differences between the position angle of each galaxy and its nearest neighbour, (c) clustering , (d) the distribution of axial ratios.

a- The observed anisotropy in the distribution of $N(\phi)$ with a peak around $\phi = 90^{\circ}$ is significant only for the galaxies with smaller angular sizes. This can be either a real effect for the more distant galaxies in this region of the sky or could be due to some undetermined biases in the position angle measurements of the smaller images.

b- The normal observational χ^2 parameter showed that the observed frequency distribution of difference between position angles of nearest neighbours in the ROE data is consistent with a uniform distribution . The excess for the 0° to 10° and 80° to 90° ranges of $\Delta\phi$ (figure 12) is due to the artificial peaks at $\phi = 0^{\circ}$ and $\phi = 90^{\circ}$.

c- The results from measurements on distant galaxies, are important for the extension of quantitative investigations of these objects out to very great distances, $z \sim 0.5$. Comparing the observed frequency distribution of angular separations of nearest neighbour of galaxies with that expected for a random distribution, we see that the galaxies are non-randomly distributed, that is, there is evidence for significant clustering. The covariance analysis gives a value for the angular extent of the clusters which allows us to obtain an approximate estimate of 6.5 galaxies per cluster. This number of galaxies in a cluster is consistent with Dodd, et al. (1975), who using a different approach to the same data, found between 2 and 6 galaxies per cluster.

d- From the observed frequency distribution of axial ratios , we found out that there are large quantization effects in the axes measurements.

We do not believe that information on intrinsic forms of galaxies can be obtained from the axial ratio distribution of all 3054 galaxies since the data are dominated by the smaller galaxies for which the quantization effects are overwhelming . If one selects only those galaxies with corrected diameters $> 100\mu m$ (7 arc sec) and corrects for the Holmberg and Opik effects a ratio of spirals to ellipticals is indicated which is consistent with that obtained by de Vaucouleurs and Van den Berg for bright galaxies (section 3.5 a) . For these galaxies there is no real excess at $r = 1$. We regard the conclusion of Dodd et al.(1975) that the peak at $r = 1$ for the smaller galaxies indicates the presence of substantial numbers of spherical and ellipsoidal galaxies as questionable. The possibility that it is solely due to quantization and selection effects in the measurements can not be ruled out.

The huge quantities of data involved make manual measurements out of the question from a practical view, not to mention bias through severe physiological , subjective and selective effects (Holmberg,1946; Opik, 1969) . It was necessary, therefore, to develope a high-speed machine capable of performing, objectively and accurately , the measurements of the properties (positions, sizes, etc.) of the very large numbers of faint images recorded on the photographs. Therefore, we turn our attention to the COSMOS machine in the next chapter.

CHAPTER 4

COSMOS DATA

4.1- General remarks

A preliminary analysis of the properties of faint galaxies recorded on the plates taken with the UK 48-inch Schmidt Telescope has already been discussed (chapter 3). Such visual measurements of images may, however, be subject to severe subjective effects (Holmberg,1946; Opik, 1969), are extremely tedious and considerably time consuming. For these reasons, the COSMOS machine was constructed at the Royal Observatory Edinburgh with the capability of carrying out large numbers of measurements of the type useful in cosmological studies (positions, sizes, transmission, orientations and shapes) objectively, accurately and at high speed. The combination of good quality, deep plates from the UK Schmidt Telescope and automatic measures from COSMOS provides a powerful system for carrying out objective measurements in cosmology.

It is the purpose of this chapter to describe the distribution of axial ratios of galaxies and also the distribution of separations between each galaxy and its nearest neighbour from the COSMOS computer output. In forthcoming pages, results obtained with the technique will be presented.

4.2- The COSMOS automatic, plate-measuring machine

COSMOS is capable of precision measurement of Co-ordinates, Sizes, Magnitudes, Orientations and Shapes of images of stars and galaxies at rates of up to 4000 images per second . The measurements are recorded on magnetic tape, which are analysed on the ICL 1906A computer at the Atlas computing laboratory.

There are three modes of operation; coarse, mapping and fine.

1. Coarse measurements

This is a raster scan in increments of about 8 μm (Pratt, et al. 1975) in which an artificial threshold can be incorporated. This enables the selection of objects greater than a certain surface brightness, and within the resolution it is possible to get rough areas and shapes. An important aspect of the coarse mode is the separation of stars and galaxies by means of a magnitude-area relation which stars obey and galaxies do not. It is therefore essential to use the coarse mode first when studying galaxies to avoid wasting time in the fine mode (see later).

The final results for the objects of interest are coordinates to $\pm$ 4 μm, and rough values for the areas and shapes. Typically the machine scans in coarse mode at 10^6 images/hour .

2. Mapping mode

This is the same type of scan as that in coarse measurement, but the output consists of a measure of the transmission to an accuracy of 1% at every 8 μm increment. This mode allows the detailed examination by off line computer analysis of areas of doubt or complexity such as bridges between galaxies or galaxies with complex structure .

3.Fine mode

This gives more precise values. When operational, it will give coordinates $\pm$ 0.5 μm, magnitudes to 0.016 and orientations to $\pm 3^{o}$. To obtain shapes and orientations the image is sampled in 1024 concentric ellipses of varing inclinations and ellipticities. Iterating on harmonic signals produced by the various shells gives the result. The speed here is about 10^{3} elongated images per hour. Fine measurement produces the type of information useful in the study of the properties of faint galaxy images (positions, sizes, shapes and orientations); it has been seen, however, that this mode of measurement is rather slow, a good deal slower than coarse measurement.

4.3- Description of COSMOS data

Galaxies are identifiable visually from stars on photographic plates by their generally tenuous appearance, odd shape and or low surface brightness. These qualities distinguishing galaxy images may similarly be used by the computer for separating the two types from COSMOS data (MacGillivray, et al. 1976) .

In coarse measurement mode of operation, the parameters obtained from the machine for each image (as our data) are the rectangular coordinates (X and Y with arbitrary zero point), the extents in the X and Y directions (in 8μm increments), the area (in 8μm X 8μm squares) detected above the threshold, and a measure for the minimum transmission (T_{min}) within the image on a scale from 1 to 128 with the darker parts having lower values. In this work, we selected only the rectangular coordinates, the extent in the rectangular coordinates, and the area for diameters greater than 100μm. These quantities are sufficient for a crude examination of the distribution of axial ratios of the images of galaxies and clustering.

4.4- Axis ratios and position angles from COSMOS data

From coarse mode data on extents, dX and dY, and image area in increments A, we are interested in determining the distributions of b/a and ϕ for various galaxies.

Getting the apparent axis ratio b/a from dX, dY and A should be quite simple if the image is truly elliptical. For convenience we list three possible situations, which we code 1-3 . By defining the area ratio as :

$$AR = \frac{dX \cdot dY}{A}$$

we consider these codes as follows:

Code 1- AR=1.00 ; the image is a perfect rectangle, and it is clearly not an ellipse. Therefore according to the code we define the angular diameter (θ =2a) and b/a as :

$$\theta = 2a = \text{Maximum of } (dX, dY)$$

$$b/a = \text{Minimum of } (dX, dY)/\text{Maximum}(dX, dY)$$

Code 2- $1.00 < AR < 4/\pi$; the image can not be elliptical, but we repeat the above analysis. It is not rectangular however.

Code 3- $AR \geq 4/\pi$; in this case, the image can be elliptical and our equations(see appendix 3) do permit us to fit an ellipse to the data.

From appendix 3 we have :

$$b/a = \frac{Z-(Z-4A/\pi)^{\frac{1}{2}}}{2}$$

$$Z - b$$

and

$$\cos\phi = \left[\frac{dX^2 - 4b^2}{4(a^2-b^2)}\right]^{\frac{1}{2}}$$

where,

$$Z = \left[\frac{dX^2+dY^2}{4} + 2A/\pi\right]^{\frac{1}{2}}$$

and ϕ is the position angle of images.

In COSMOS data, we sometimes encountered images for which AR $<$ 1 , these are termed "mistakes" . We ignored them in our consideration.

4.5- Quantization effect in the COSMOS data

This effect is present in the COSMOS data, that is both position (X and Y) and axes (a and b) are given to the nearest 8 μm, but this effect should generally vanish as diameter increases.

4.6- True values of a, b/a and ϕ by COSMOS data and formula

We need to investigate how accurately the COSMOS data (dX, dY and A) and formula (in appendix 3) can reproduce the true values of major axis (a), axial ratio(b/a) and position angle(ϕ). We can say that this will depend upon :

1. The true value of a (computations show that for larger a the calculated values will become more accurate).

2. The true value of position angle (ϕ).

3. The true value of axial ratio (b/a).

4. The position of the centre of the galaxy with respect to the grid.

A square grid representing the 8μm X 8μ m grid of COSMOS was taken and overlays of ellipses with semi-major axes scaled to represent a=25μm, 50μ m and 100μ m and with 5 values of axial ratio b/a were superimposed. The position angles ϕ of the ellipses and the positions of the centres of the ellipses relative to the grid were varied. For each position angle and position of centre the corresponding values of Δx, Δy and A were determined. The formula of section 4.4 were then used to obtain calculated values of a, b/a and ϕ to compare with the true values.
Table VII gives the results for a=50μ m and the ellipses centred on a vertex of the grid (position 1).

Table VIII

Calculated values of a, b/a and ϕ by using true values of a, b/a, ϕ and measured values of Δx, Δy and A .

True values		Measured values			Code	Calculated values		
b/a	ϕ^0	Δx	Δy	A		a	b/a	ϕ^0
0.1	0	2	8	16	1	32.00	0.25	0.25
	10	2	10	12	3	40.34	0.15	7.52
	20	4	10	12	3	42.70	0.13	20.68
	30	6	10	14	3	46.14	0.13	30.41
	40	8	10	16	3	50.82	0.13	38.45
	45	8	8	8	3	45.11	0.08	45.00
0.3	0	4	12	40	2	48	0.33	0.00
	10	4	12	38	2	48	0.33	0.00
	20	6	12	40	3	51.26	0.31	21.65
	30	8	10	36	3	48.99	0.31	37.32
	40	8	10	36	3	48.99	0.31	37.32
	45	10	10	38	3	57.77	0.26	45.00
0.5	0	6	12	64	2	48	0.5	0.00
	10	6	12	62	2	48	0.5	0.00
	20	8	12	64	3	51.94	0.48	25.88
	30	8	12	62	3	52.41	0.46	26.89
	40	10	10	62	3	50.82	0.49	45.00
	45	10	10	64	3	50.27	0.52	45.00
0.7	0	8	12	84	2	48	0.67	0.00
	10	10	12	86	3	53.04	0.62	32.93
	20	10	12	90	3	51.20	0.70	29.15
	30	10	12	90	3	51.20	0.70	29.15
	40	10	12	86	3	53.04	0.62	32.93
	45	10	10	82	2	40	1.00	90.00
1.0	0	12	10	120	2	48	1.00	90.00

From the table it can be seen that except for two cases the calculated $\underline{a}$ is within 10 μm of the true value of 50 μm and the calculated b/a is within 0.1 of the true value. Similar results were obtained for ellipses centred on the mid point between two vertexes of the grid(position 2) and the mid point of a grid square (position 3). For position 2 no calculated values of $\underline{a}$ and b/a lay outside the above limits while for position 3 there were again 2 cases outside these limits. In general it can be said that if the galaxy images are indeed ellipses the COSMOS coarse mode measurements of Δx, Δy and A should allow the axial ratios of galaxies with a $> 50\,\mu$m to be determined with sufficient precision to justify a study of their distribution . On the other hand, it can be seen that errors in the determination of the position angles ϕ are large. There is also an ambiguity in the sign of ϕ . We conclude that coarse mode measurements can not be used for position angle measurements.

For a = 25 μm the calculated values of a differ by up to 15 μm while the discrepancy between true and calculated b/a may reach 0.3 . For a=100 μm all calculated values are within 5 μm and b/a are within 0.05 of the true value.

4.7- Observed and expected distributions of axial ratios

For the galaxies recorded by COSMOS in an area 7.37 cm X 7.37 cm (1.37° X 1.37°)on plate R1049* the values of 2a and b/a were calculated from the data on extents and image areas. We then selected 936 galaxies with diameters 2a $\rangle$ 100 μm . The quantization effects should be negligible for such images.

Using the frequency distributions of true axial ratios for ellipticals and spirals (Sandage, et al. 1970) we can calculate the corresponding frequency distributions of apparent axial ratios(b/a). Figure 20 shows these distributions, each normalized to a total of 936, together with the frequency distribution of COSMOS axial ratios. (For brevity we shall refer to the values of b/a calculated by us from the extents and image areas measured by COSMOS as 'COSMOS axial ratios' . We recognize that there will be errors in b/a for any images that are not filled ellipses).

Without the need to calculate χ^2 it can be seen immediately that there is no mixture of ellipticals and spirals that will give a fit to the distribution of COSMOS axial ratios. The latter shows a strong peak at around b/a =0.5 and very few near circular galaxies.

---

* The parameters of the plate are as follows :

Date :	1974 December 8
Plate number :	R1049
Emulsion :	Eastman Kodak 098
Filter :	Schott RG 630
Exposure :	60 min
Plate Centre(1973-5):	RA 02^h42^m , Dec $-29^{\circ}\ 54'$
Plate Scale :	67 arcsec. mm^{-1}

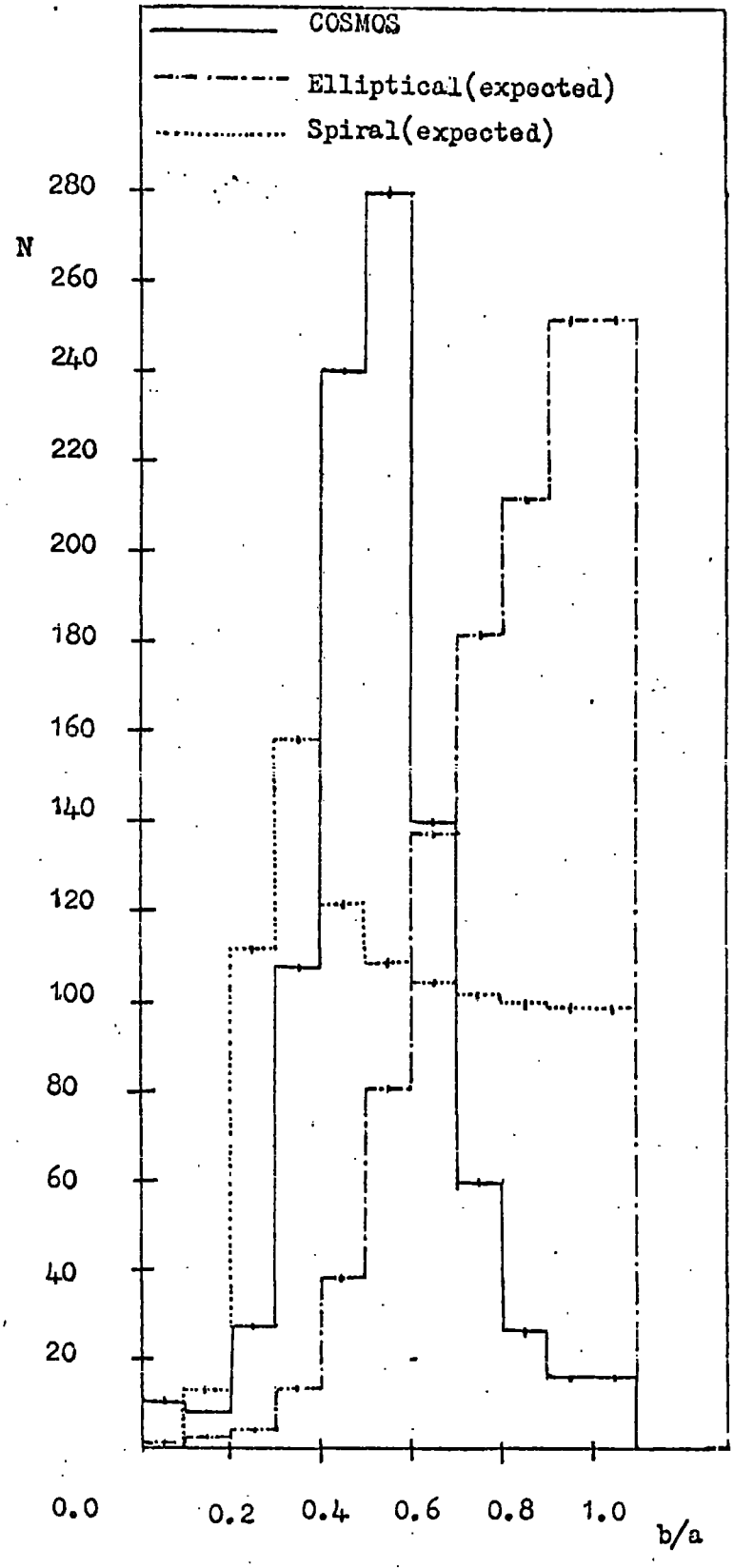

Fig.20 - Comparison of the distribution of COSMOS axial ratios for 936 galaxies with $2a > 100\mu m$ with the expected distributions for spirals and ellipticals.

4.8- Optical verification of COSMOS data

As we were unable to explain the observed histogram of COSMOS axial ratios with any mixture of spirals and ellipticals we checked similar distributions for stars to ensure the data and reduction techniques were correct .

According to section (4.4), for our convenience we listed three possible situations, which we coded 1-3 . The computer program was run for stars on the tapes for J149,R1049 and J1916 plates. The results have been given as follows (Ellis, private communication) ·

Distributions of axial ratios for stars also show a marked absence of circular stars, and an overwhelming preference for objects with $b/a \approx 0.5$. This is observed for large ($2a > 100\mu m$) and small ($2a < 100\mu m$) stars on all 3 plates.

The first possible reason, namely diffraction spikes (which increase the extents considerably, but not the area) is discounted by several results :

1) Small stars do not have spikes.

2) The effect would depend on size and brightness of the star. There is no correlation with size or minimum transmission.

3) Extent (dX,dY)ratios should be more or less 1 and there should be little difference between dX/dY and dY/dX, yet this is not so .

The extent ratios are in fact interesting. On all three plates for both sizes there are at least twice as many star images elongated in the X direction. Physically this can not be explained.

The second possible interpretation of these curious results is that the extents and areas are affected by the $8\mu m$ COSMOS quantization .

However above $2a \sim 50\mu m$ this has virtually no effect on b/a or dX/dY. In fact this explanation can clearly be discounted since the effect would decrease with increasing size and it does not do so. The problem is vital to those using COSMOS data and should be rectified immediately.

To investigate these results further it was decided that direct measurements of the area of the plate R1049 scanned by COSMOS should be made. Accordingly the plate was obtained on loan from R.O.E. The remainder of this section is concerned with the preliminary results of measurements at Durham by the author and his colleagues. These measurements will continue in greater detail.

The equipment used was an Olympus Stereo Microscope with magnification continuously variable between X10 and X40. The eyepiece scale covers an area of 1 cm^2 at X10.
The smallest scale division corresponds to $25\mu m$ at X40 magnification. In theory, sizes of objects could thus be estimated to within $10\mu m$. The diffuseness of most galaxy images, however, made it difficult to estimate sizes to better than $25\mu m$. The microscope was mounted on a coordinatograph which allowed slow motion movement along two axes accurately at right angles. The coordinatograph was designed for automatic electronic digital read out, however, and the coordinates could be set by hand only to an accuracy of $\pm 250\mu m$.

From the known pattern of bright stars on the scanned area the conversion constants from COSMOS to Durham coordinates were determined.

A list was prepared from the COSMOS magnetic type of all objects for which the calculated 2a $\geq$ 200 μm. There was a total of 62 . Each object in turn was searched for at the position indicated by COSMOS. Even allowing for the setting error of $\pm$250 μm it should have been posible unambiguously to identify objects of this size . In fact 38 were identified. For each of the remaining 24 objects there was no galaxy within the setting error distance down to one third of the recorded size. In 12 cases there was a star within the the setting error distance but, bearing in mind that in the other 12 cases there was no large object at all, one can not be sure that COSMOS had recorded that star as a galaxy. Of the 38 identifications one was apparently a plate fault, and 24 were elliptical single galaxy images for which the calculated COSMOS axial ratio should have been correct. Details of these are given in table 9 . The remaining 13 were complex objects : 9 were close pairs of galaxies which COSMOS had treated as a single object and 2 were groups of 3 galaxies.

Turning to the 24 galaxies listed in table 9 one sees that the COSMOS axial ratios are systematically smaller than the directly measured ones and never exceed 0.6. This would be accounted for if the COSMOS extents were too large or the image areas too small. For the largest galaxy in table 9 the COSMOS values are dX=1000 μm, dY = 240 μm while the measured values were dX = 550 μm and dY =325 μm. For the other galaxies the discrepancies are smaller, the COSMOS extents being on average 15% larger than the Durham measured extents. It seems then that the problem is mainly that the recorded image areas are too small.

Table IX

COSMOS coordinates and extents, calculated angular diameter and b/a, and measured angular diameter and b/a, for all unambiguously identified single galaxies with 2a $\geq$ 200 μm (all dimensions in microns).

COSMOS				Calculated		Measured	
X	Y	dX	dY	2a	b/a	2a	b/a
121899	67659	168	240	271	0.41	175	1.0
118084	55085	160	216	234	0.57	225	0.56
117816	23413	272	240	352	0.24	325	0.31
112524	59206	184	176	222	0.56	175	0.86
110281	36789	216	192	269	0.39	175	0.71
109862	57746	192	128	204	0.53	150	0.67
107652	75900	200	152	218	0.58	175	1.0
106483	71937	1000	240	1000	0.03	600	0.42
98178	54215	224	208	288	0.36	225	0.33
92707	40574	136	184	218	0.32	250	0.30
92275	79989	120	216	235	0.33	225	0.56
91871	29258	184	176	225	0.53	100	0.75
91674	25545	184	208	262	0.36	150	0.50
87338	57162	120	192	217	0.31	150	0.33
83296	73230	176	224	258	0.47	100	0.75
79934	20154	224	152	241	0.51	75	1.0
78172	69235	240	200	276	0.53	175	0.71
69628	40906	232	216	281	0.52	100	0.75
68168	37218	256	112	267	0.31	225	0.22
65796	52782	176	152	207	0.51	100	1.0
61460	43938	168	144	203	0.44	175	0.71
59622	55591	256	248	341	0.31	200	0.38
57498	36696	272	552	607	0.16	550	0.18
53495	89459	280	144	294	0.38	150	0.67

While the check of the 2a $>$ 200μm objects was being done it was noticed that there were some large galaxies not recorded by COSMOS. A systematic scan of the area for all objects with 2a $>$ 400μm revealed 5 clear galaxies. Only 2 of there had been recorded as galaxies by COSMOS.

One must conclude that for large galaxies ($>$ 200μm) the COSMOS data from plate R1049 are unreliable . About 30% of the objects recorded are not present and some real objects are missed. About 20% are pairs or groups of galaxies not resolved in the coarse mode measurement. The recorded values of extents and areas of the single elliptical galaxy images give calculated axial ratios systematically smaller than the true values.

This may not be important if the smaller galaxies are measured correctly since they greatly outnumber the larger ones. There are on average 17 galaxies per cm^2 with 2a $>$ 100μm. For selected 1cm X 1cm areas the positions of all galaxies with calculated 2a $>$ 100μm were plotted. The centres of the microscope scale having been set by hand to within 250μm of the centre of the square it was possible to recognize the pattern of galaxies and to line up the scale such that coordinates could be measured to within 10μm. In this way it is possible to check the COSMOS data over the whole 53 cm^2 scanned area . The results of measurements of 4 cm^2 are as follows ·

In the 4 cm^2 area COSMOS recorded 71 galaxies with calculated 2a $>$ 100μm, of these 60 were found to be single galaxy images, 2 were doubles and one was a triple galaxy with components separated by $<$ 100μm . There was one identification with a star and 2 with parts of the diffraction spikes of bright stars. The remaining 5 objects could not be seen. They were grouped together in a 2 mm^2 area and had recorded extents up to 872μm. They appear to be spurious.

For the 60 single galaxies the mean X extent from COSMOS was 104.9 μm and the mean Y extent was 105.1 μm. There is thus no bias to larger X extents for these galaxies. Our measured mean extents were 104.6 μm and 99.0 μm in the X and Y directions respectively. The agreement of the extents is better for these than for the larger galaxies . In Fig.21 are plotted the calculated COSMOS axial ratio versus the directly measured axial ratio for all 60 galaxies . Again the COSMOS values are systematically lower so that it seems that the image areas are again too small. Figure 22 shows the distributions of COSMOS and directly measured axial ratios. The directly measured ratios show the effective quantization of the axes into 25 μm increments. The COSMOS distribution follows that given in Figure 20 for all 936 galaxies.

The indication is that the COSMOS data are considerably more reliable for objects with 100 μm $< 2a <$ 200 μm than for the larger objects with regard to the identification of single galaxies and the X and Y extents. Unfortunately one must conclude that the coarse mode measurements of extents and image areas can not be used to infer the axial ratios for any size.

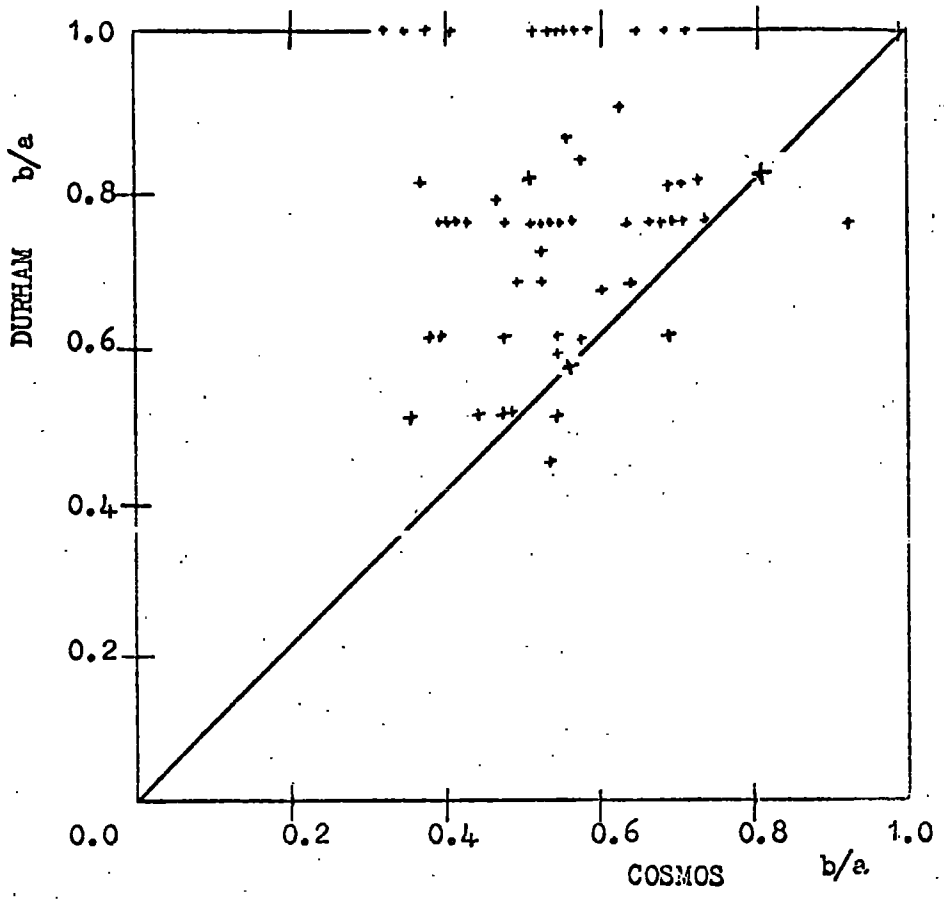

Fig.21 - Comparison of COSMOS axial ratios with those measured at Durham.

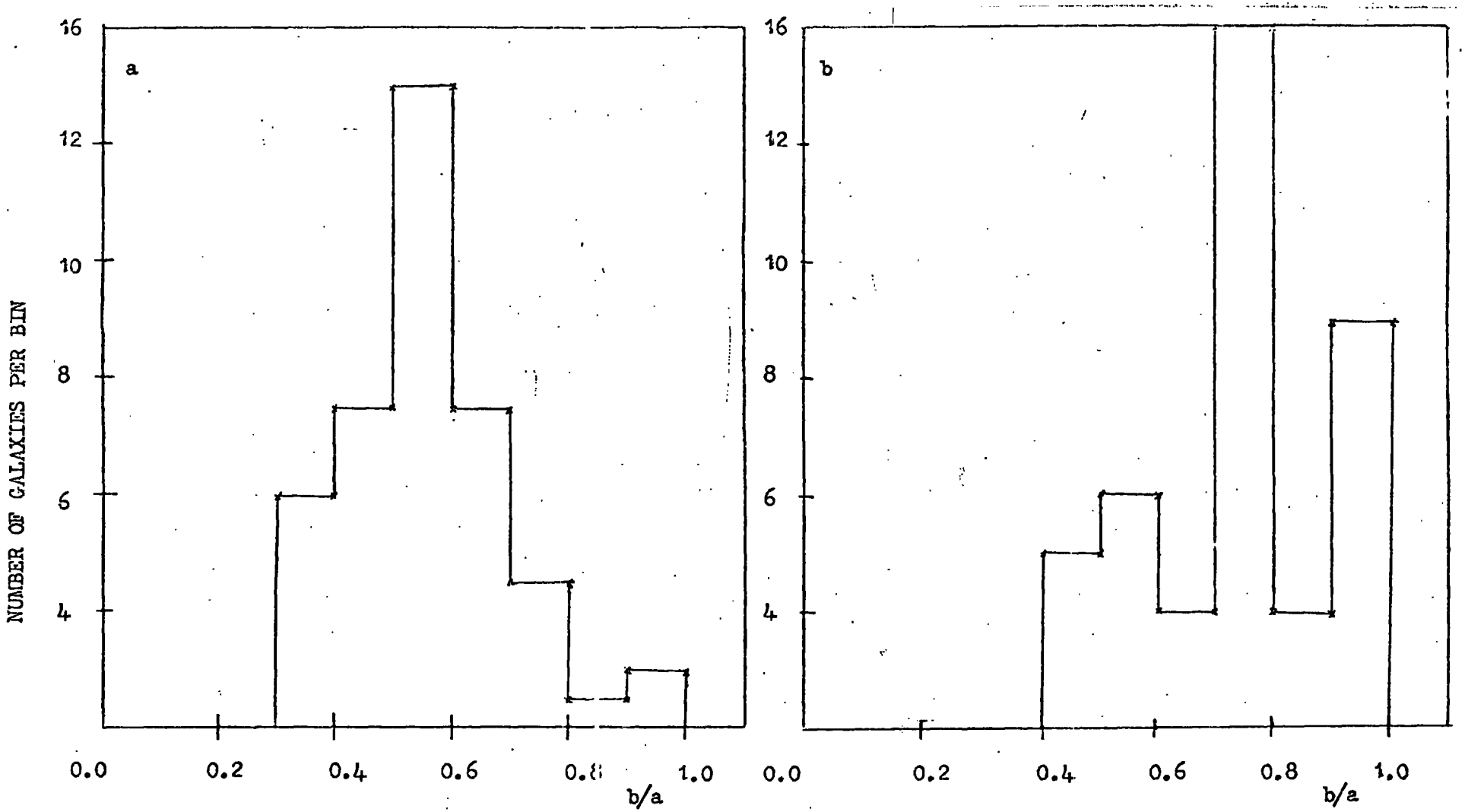

Fig.22 - Frequency distribution of apparent axial ratios for 60 galaxies,
(a) COSMOS axial ratios (b) Measurements at Durham.

4.9- Distribution of nearest neighbour separation

The observed frequency distribution of nearest neighbour separations for 936 galaxies with 2a $\geq$ 100 μm from COSMOS data is shown in Figure 23. Separations between mutual nearest neighbour are counted twice. Also shown is the predicted distribution (see appendix 1a) for a random distribution of galaxies on the sky assuming an average density of galaxies per unit area equal to that observed. There is no need to consider quantization of position in this case.

The observed distribution shows an excess at small separations. The excess in the first bin is in fact greater than that shown since, as we have seen, COSMOS will treat pairs of galaxies as one when the separations are $\leq$ 100 μm. Again the clustering of galaxies is confirmed.

Although a covariance function analysis has been done for the COSMOS data from this plate it was for galaxy images down to smaller size limits so that an estimate can not yet be made of the mean number of galaxies in a cluster. In the present distribution, for galaxies with 2a $\geq$ 100 μm, the excess occurs for separations 800 μm (54 arcsec). In the ROE data which includes all galaxies with 2a $\geq$ 50 μm the excess occurs for separations $<$ 400 μm. This indicates that the metric size of the clusters is similar for the two sets of observations.

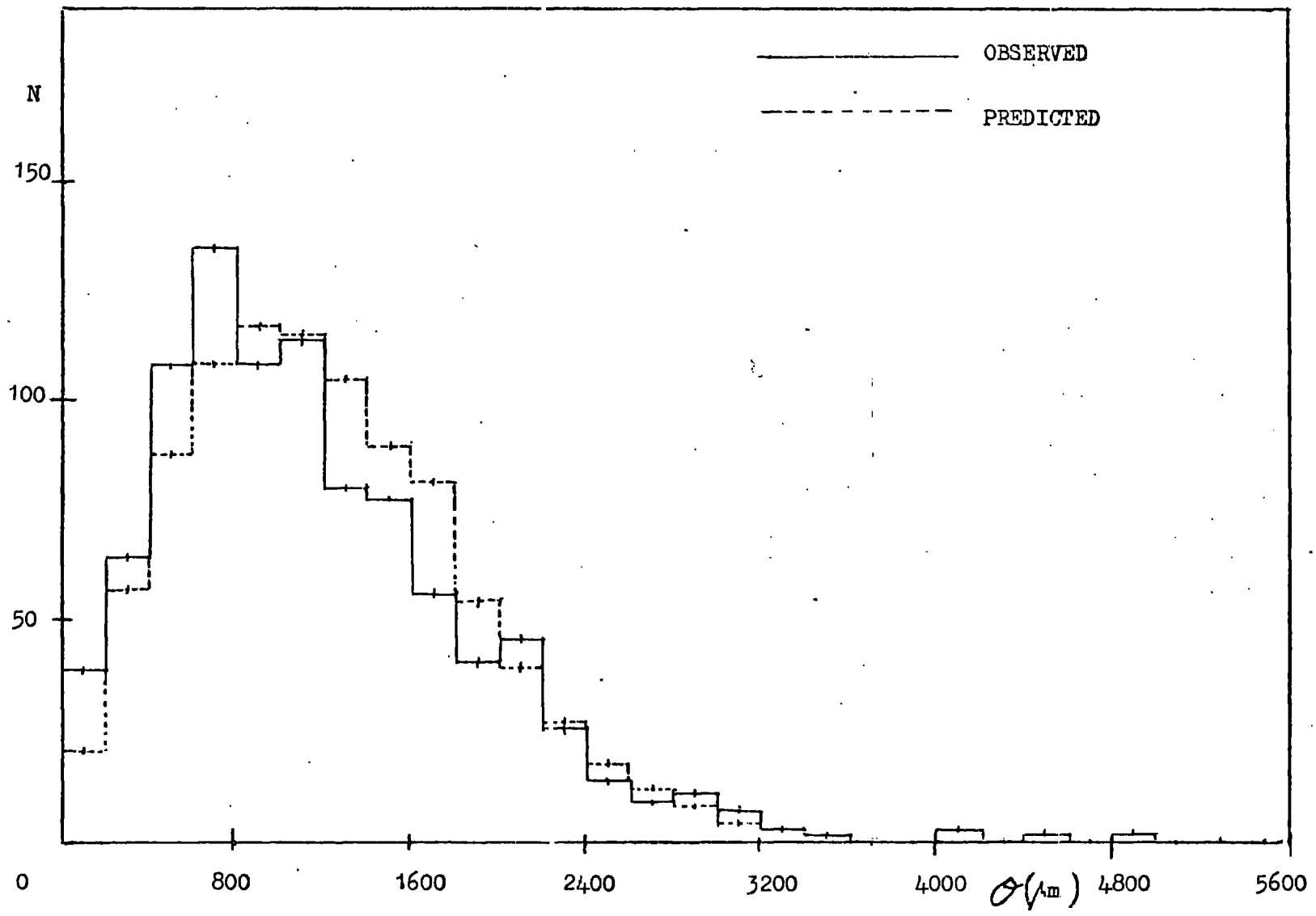

Fig.23 - Distribution of nearest neighbour separations for 936 galaxies with 2a > 100 μm

CHAPTER 5

GENERAL CONCLUSIONS AND DISCUSSION

5.1- General remarks

In recent years considerable advances have been made towards an understanding of the origin and evolution of galaxies in the Universe. On the theoretical side two theories in particular have been developed to the point where confrontation with observation is possible; these are the theories of Gravitational Instability and Cosmic Turbulence(Jones, 1976).

The distribution of angular momenta of the members of great aggregations of galaxies can be used to distinguish between these and other theories. Because of the lack of suitable material previous analyses of this kind have reached conflicting conclusions.

With the advent of COSMOS however, many of the problems eg. subjective biasses, will be overcome. In the fine mode of operation the prospects for testing the theories are excellent. In this work we have not only studied the position angle distributions but also those of axial ratios. The latter are more difficult to interpret in terms of a non-random three-dimensional distribution of angular momentum because the interpretation requires a knowledge of the mixture of spirals and ellipticals. It would thus be essential first to separate the different galaxy types before discussing non-randomness. Having said that, however, studying the axis ratios is important since it is only by using position angles and axis ratios together that one can be sure a non-random distribution is physical and not due to measurement problems.

5.2- Frequency distribution of position angles

There are few catalogues that record position angles for large numbers of galaxies.

Brown's results(1964, 1968) concerning the distribution of orientation angles of spiral galaxies in different areas of the sky have been discussed and various statistical tests were applied. Brown moved galaxies to make the histogram smoother and found strong skew distribution of position angles. Our work shows the smoothing was unnecessary and has significantly altered the histograms. However, even with the raw data there are several fluctuations significant at the 2σ level and two above the 4σ level. A detailed investigation of the galaxies in these large peaks failed to give more evidence for a physical non-randomness. Moreover, when the total number of possible histograms was computed the two events become hardly significant(a probability of 1 in 8.8 of it having occurred by chance).

It is apparent from frequency distribution of position angles for 854 galaxies in the ROE data, that there are large peaks at $\phi = 0^{\circ}$ and $\phi = 90^{\circ}$ in 1°bins, and that there are subsidiary peaks at multiples of 10°in ϕ (Figure 10). This clearly is due to the observer having measured to different accuracies for different sizes, After summing the data into larger bins to take account of this, some anisotropy in the frequency distribution of orientation angles(Figure 11, solid lines) remains for the galaxies with smaller angular sizes. This anisotropy could be a real effect for the more distant galaxies, or it could be due to some undetermined biasses in determining their orientation angles.

The relatively small excess for the 0° to 10° and 80° to 90° ranges of the observed histogram of the difference between orientations of nearest neighbour galaxies (Figure 12) can be accounted for by to the artificial peaks at $\phi = 0^{\circ}$ and $\phi = 90^{\circ}$ in the $N(\phi)$ distributions.

5.3- Nearest-neighbour results

Comparing the observed frequency distribution of angular separations of nearest neighbour of galaxies in both the ROE and COSMOS data with that expected for a random distribution, we found that there is good evidence for clustering. A recent analysis of the distribution of galaxies on a deep IIIaJ Schmidt Telescope plate (Dodd, et al. 1975) has shown that the results are consistent with the hypothesis that all galaxies are contained in clusters containing from 2-6 members. By using the covariance analysis (Dodd, et al. 1976) that gives a value for the angular extent of the cluster we obtained an approximate estimate of 6.5 galaxies per cluster, which is consistent with the results of Dodd, et al.(1975).

5.4- Frequency distribution of axial ratios

The frequency distributions of apparent axial ratios of galaxies depend upon the distribution of true axial ratios and upon any anisotropies in the three-dimensional distribution of angular momentum vectors. In interpreting the axial ratios, because we have found no strong evidence for anisotropies in position angle, we have assumed a random distribution of angular momentum vectors. It is should then be possible to investigate the distribution of true axial ratios and hence to estimate the relative numbers of elliptical and spiral galaxies in our samples of distant galaxies.

There are large quantization effects in the both major and minor axes measurements in the ROE data. After these were allowed for the fraction of spirals to ellipticals for the large galaxies was found to be consistent with that obtained by de Vaucouleurs(1963) and Van den Bergh(1975) . The peak at b/a =1 for the smaller galaxies (mentioned by Dodd, et al. 1975) is due to quantization and selection effects in the measurements.

From the COSMOS data it should also be possible to obtain a distribution of axial ratios. In the coarse mode the value of b/a is not directly measured but should be calculable for images that are filled ellipses from the recorded X and Y extents and image areas. The COSMOS axial ratios however have a distribution peaking at b/a = 0.5 and strong deficit near b/a =1 .
This distribution can be reproduced by no mixture of spiral and elliptical galaxies. The need for a visual check of the data was thus indicated.

5.5- Visual check of an area measured by COSMOS

Only preliminary results concerning the visual check of the area of plate R1049 measured by COSMOS are at present available. Nevertheless they are of some interest. All recorded nonstellar objects with $2a > 200\,\mu m$ have been checked over the total scanned area and objects with $2a > 100\,\mu m$ have been checked over 4 cm^2. For both groups the measured axial ratios are nearly always longer than the COSMOS axial ratios but there is otherwise little correlation between the two. It is concluded that the coarse mode data can not at present be used to determine the axial ratios and further work must make use of the fine mode facilities of the machine . There are indications that this may be due to the recorded image areas being too small. For the larger galaxies there are some important discrepancies between the visual and COSMOS measurements. These have been discussed in chapter 4 . COSMOS appears to be generating a significant number of spurious objects and has missed some of the largest clear galaxies. For the smaller galaxies there is much better agreement between the measurements. It is important to extend these investigations to see, for instance, whether the use of the coarse mode data for covariance analysis of galaxy clustering is justified. Further tests would include, increasing the area over which checks of $2a > 100\,\mu m$ objects have been made and then extending the checks to still smaller objects. It is important to account for the assymmetry in the recorded X and Y extents for stars. A systematic visual scan of at least part of the area for all objects with, say, $2a > 50\,\mu m$ should be made to see whether COSMOS is missing a significant proportion of all the galaxies or just the largest ones. This is probably the most important check as far as the covariance analysis is concerned.

ACKNOWLEDGEMENTS

I would like to thank my supervisor, Dr. J.L.Osborne for his help and encouragement during this time of research leading to this thesis, and Dr. R.S.Ellis for his many helpful suggestions and discussions.

I would like to thank Professor A.W.Wolfendale for making available the facilities of the Department of Physics of the University of Durham.

U.K.S.T.U. are thanked for supplying the photographic plates and the Royal Observatory Edinburgh are thanked for providing the COSMOS data. With regard to the latter I am particularly indebted to Dr. H.MacGillivray for helpful discussion and loan of his thesis.

Finally, I would like to thank the Ministry of Science and Higher Education, Iran and the University of Ferdowsi, Meshed, Iran for their financial support.

REFERENCES

Brown, F.G., 1938. Mon. Not.R. astr. Soc., 99 , 534 .

Brown, F.G., 1964. Mon. Not. R. astr. Soc., 127, 517 .

Brown, F.G., 1968. Mon. Not. R. astr. Soc., 138 , 527 .

Corben, P.M., Reddish, V.C. and Sim, M.E., 1974. Nature, 249 , 22 .

Dodd, R.J., Morgan, D., Nandy, K., Reddish, V.C. and Seddon, H., 1975. Mon. Not. R. astr. Soc., 171 , 329 .

Dodd, R.J., MacGillivray, H.T., Ellis, R.S., Fong, R. and Phillipps,S., 1976. Mon. Not. R. astr. Soc., 175 , 33p.

Hawley, D.L. and Peebles, P.J., 1975. Astron. J., 80 , 477 .

Holmberg, E., 1946. Lund. Medd. Ser. 2, No. 117 .

Hubble, E.P., 1926. Astrophys. J., 64 , 321 .

Hubble, E.P., 1936. The realm of the nebulae, New York, Dover Publications.

Jones, B.J.T., 1976. Rev. Mod. Phys., 48 , 107 .

Kristian, J., 1967. Astrophys. J., 147 , 864 .

MacGillivray, H.T., 1975. PhD Thesis, Department of Astronomy, University of Edinburgh.

MacGillivray, H.T., Martin, R., Pratt, N.M., Reddish, V.C., Seddon, H., Alexander, L.W.G., Walker, G.S. and Williams, P.R., 1976. Mon. Not. R. astr. Soc., 176 , 265 .

Neyman, J. and Scott, E.L., 1952. Astrophys. J., 116 , 144 .

Opik, E.J., 1923. Observatory, 46 , 51 .

Opik, E.J., 1969. Irish Astr. J., 8 , 229 .

Opik, E.J., 1970. Irish Astr. J., 9 , 211 .

Ozernoi, L.M., 1974. The Formation and Dynamics of Galaxies, IAU Symp. 58 , 85 .

Peebles, P.J.E., 1970. Astron. J., 75 , 13 .

Pratt, N.M., Martin, R., Alexander, L.W.G., Walker, G.S. and Williams, P.R., 1975. Image Processing techniques in astronomy, P.217, Reidel Publishing Company, Dordrecht.

REFERENCES

Reaves, G., 1958. Publ. Astron. Soc. Pacific, 70 , 461 .

Reinhardt, M., 1971. Astrophys. and Space Sci., 10, 363 .

Reinhardt, M., 1972. Mon. Not. R. astr. Soc., 156 , 151 .

Reinhardt, M., 1973. Preprint On the distribution of Angular Momenta of Galaxies.

Reynolds, J.H., 1920. Mon. Not. R. astr. Soc., 81 , 129 .

Sandage, A., Freeman, K.C. and Stokes, N.R., 1970. Astrophys.J., 160 , 31 .

Van den Bergh, S., 1975. R.A.S.C.J., 69 , 67 .

Vaucouleurs, G. de. 1957. Aun. Obs. Le. Houga II fasc. 1 .

Vaucouleurs, G. de. 1959. Astrophys.J., 130, 728 .

Vaucouleurs. G. de. 1963. Astrophys.J. Suppl.. 8 . 31 .

Vaucouleurs, G. de. 1971. Publ. astr. Soc. Pacific, 83 , 113 .

Vaucouleurs, G. de. 1974. The Formation and Dynamics of Galaxies IAU Symp. 58 , 1 .

Vaucouleurs, G. de, and Vaucouleurs, A. de. 1964. Reference Catalogue of Bright Galaxies, Austin, Univ. of Texas Press.

Wyatt, S.P., Jr. and Brown, F.G., 1955. Astron.J., 60 , 415 .

APPENDIX 1

Expected distribution of separation of nearest neighbour galaxies for a random distribution of individual galaxies

a) No quantization of position measurements

We take a ring with radius θ and width $d\theta$. If we assume that ρ is the average number of galaxies per unit area, the expected number of galaxies in the area ($\pi\theta^2$) enclosed by the ring would be $\rho\pi\theta^2$. The probability of there being no galaxies in this area is $\exp(-\pi\rho\theta^2)$.

The probability of the distance to the next neighbour lying between θ and $\theta + d\theta$ is given by the product of the probability that no galaxies lie in the circle of radius θ and the probability that one galaxy lies in the ring of width $d\theta$,ie.,

$$P(\theta)d\theta = \exp(-\pi\rho\theta^2)\ 2\pi\rho\theta d\theta$$

and, the probability of a separation between θ_1 and θ_2 is :

$$P(\theta)d\theta = \int_{\theta_1}^{\theta_2} \exp(-\pi\rho\theta^2)\ 2\pi\rho\theta\, d\theta$$

$$= \exp(-\pi\rho\theta_1^2) - \exp(-\pi\rho\theta_2^2)$$

Therefore, multiplying the total number of galaxies in the data by above number, we find the expected number of nearest neighbour galaxies without quantization in position.

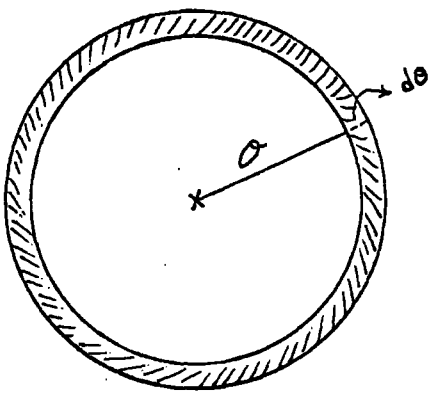

b) With quantization of position measurement

When the positions of galaxies are quantized , as in the ROE data, the derivation of the expected distribution of separations of galaxies on the hypothesis of a random distribution of galaxies on the photographic plate is as follows.

Consider the area of the plate devided into a number of square cells each having sides of length S. The expected number of galaxies in one cell is ρS^2 and the probability of there being no galaxies in a given cell is $\exp(-\rho S^2)$. The recorded position of a galaxy will be that of the centre of the cell in which it falls. If nearest neighbour galaxies are both in the same cell their recorded separation, θ_R will be zero. If nearest neighbour are in adjacent cells $\theta_R = S$ and so on . The possible values of θ_R and the number of cells having that separation from a given cell, $N(\theta_R)$ can be easily assertained by drawing out a square grid. The possibility that the recorded nearest neighbour separation in θ_R is given by the probability that there are no galaxies in the cells with separation $\langle\theta_R$ minus the probability that there are no galaxies in the cells with separation $\lesssim\theta_R$, ie.,

$$P(\theta_R)=\exp(-N(\langle\theta_R)\rho S^2)- \exp(-N(\lesssim\theta_R)\rho S^2)$$

For the ROE data :

$$S = 254\,\mu m \qquad \rho S^2=0.03393$$

and the probabilities for the first few values of θ_R are listed in the following table:

σ_R / s	$N(\sigma_R)$	$P(\sigma_R)$
0	1	0.0334
1	4	0.1227
$2^{\frac{1}{2}}$	4	0.1071
2	4	0.0935
$5^{\frac{1}{2}}$	8	0.1529
$8^{\frac{1}{2}}$	4	0.0622
3	4	0.0543

APPENDIX 2

****

Frequency distribution and frequency function equations

Schematically, we assume an elliptical contour for the galaxy drawn in cross section through the centre O at right angles to its plane in the direction of the observer, SE or OE' being the line of sight, OY the polar axis of the galaxy. (See Figure A1).

Let OE' be the line of sight to the observer, making an angle i (inclination) with OX or major axis and let OR be perpendicular to SE. SE is a tangent to ellipse , parallel to and at a distance B from OE' . The apparent axis ratio is determined by b/a, which, for various values of angle i, ranges from b to a .

The problem is to determine the apparent inclination (i) in terms of apparent and true axial ratios. If we write equation of tangent, SE , as follows:

$$y=-x\,tg\ i + \sqrt{a^2 tg^2 i + B^2}$$

where $y_o = a^2 tg^2 i + B^2$ is the intercept of the tangent on the Y-axis.

In triangle OO'R we can write $b = y_o \cos i$

or $$b^2 = y_o^2 \cos^2 i$$

$$b^2 = (a^2 tg^2 i + B^2)\cos^2 i$$

$$b^2 = a^2 \sin^2 i + B^2 \cos^2 i$$

$$b^2 = a^2 \sin^2 i + B^2(1-\sin^2 i)$$

$$b^2 = a^2 \sin^2 i + B^2 - b^2 \sin^2 i$$

$$b^2 - B^2 = \sin^2 i (a^2 - B^2)$$

If we divide above equation by a^2, we would have :

$$b^2/a^2 - B^2/a^2 = \sin^2 i\,(1 - B^2/a^2)$$

As we know :

$$r = b/a \ , \ r_o = B/a$$

Therefore,

$$r^2 - r_o^2 = \sin^2 (1 - r_o^2)$$

$$\sin i = \left[(r^2 - r_o^2)/(1-r_o^2) \right]^{\frac{1}{2}}$$

As we said in context : $F(i) = \sin i$

then

$$F(r) = \left[(r^2 - r_o^2)/ (1-r_o^2) \right]^{\frac{1}{2}}$$

is frequency distribution of apparent axial ratio.

We can take frequency function equation by differentiating equation of frequency distribution as follows :

$$f(r) = d/dr \ (F(r))$$

$$f(r) = d/dr \left[(r^2 - r_o^2) / (1-r_o^2) \right]^{\frac{1}{2}} =$$

$$\tfrac{1}{2} \left[2r(1-r_o^2)/(1-r_o^2) \right] \left[(r^2 - r_o^2) / (1-r_o^2) \right]^{-\frac{1}{2}}$$

then :

$$f(r) = r \left[(r^2 - r_o^2)(1-r_o^2) \right]^{-\frac{1}{2}}$$

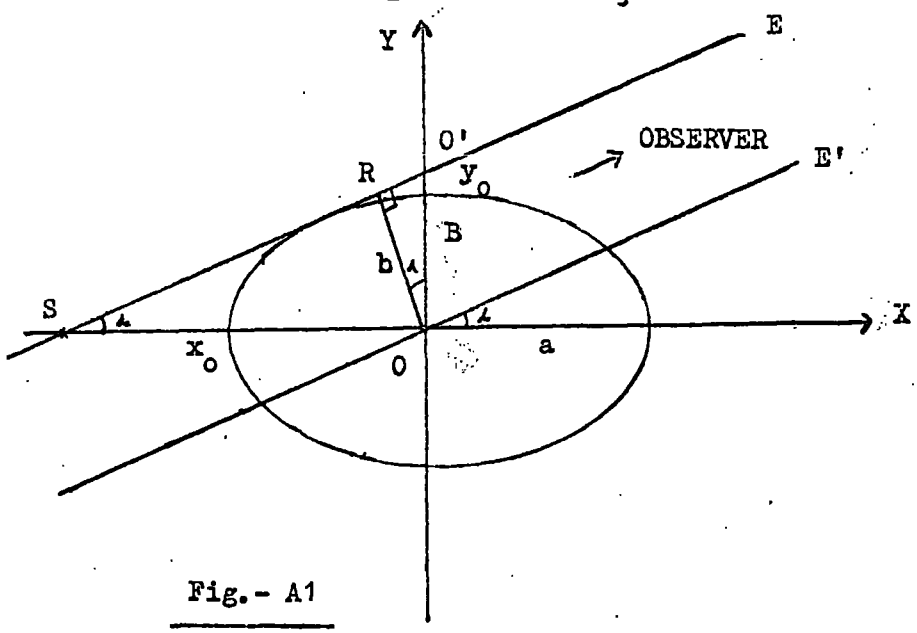

Fig.- A1

APPENDIX 3

Getting axial ratio(b/a) and position angle (ϕ) from COSMOS data

If we suppose the image is truly elliptical, we can find the axial ratio and position angle by aid of geometry as follows:

We construct two axes x' and y' for the ellipse and write down the elliptical equation :

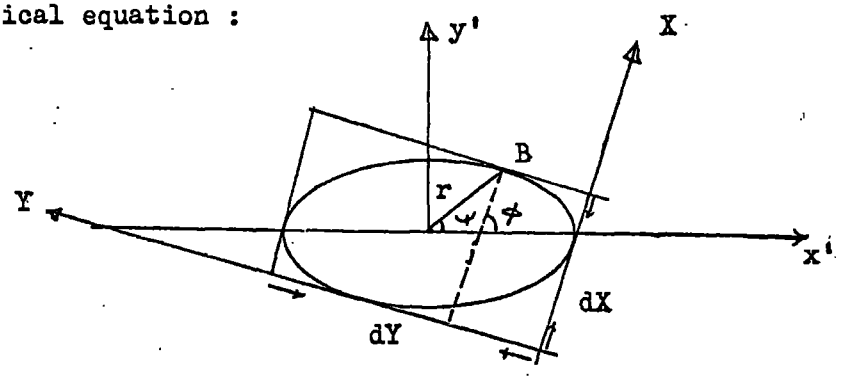

$$f = x'/a^2 + y'/b^2$$

By differentiating the above relation, we have :

$$\partial f/\partial x' = 2x'/a^2 \quad , \quad \partial f/\partial y' = 2y'/b^2$$

so $$tg\phi = y'/x' . a^2/b^2$$

In terms of COSMOS axes (X,Y)we are able to write :

$$dX = 2r\cos(\phi - \psi) = 2\left[x'\cos\phi + y'\sin\phi\right]$$

where r is the distance between point B and centre of ellipse, but

$$x' = y'/tg\phi . a^2/b^2 \quad \text{or} \quad y'^2 = \left[\frac{a^2}{b^4 tg^2\phi} + \frac{1}{b^2}\right] = 1$$

hence ;

$$dX = 2y'\left[\sin\phi + a^2\cos\phi/b^2 tg\phi\right] = 2\left[a^2\cos^2\phi + b^2\sin^2\phi\right]^{\frac{1}{2}} \quad (1)$$

Similarly for dy, we have :

$$dy = 2\left[a^2\sin^2\phi + b^2\cos^2\phi\right]^{\frac{1}{2}} \quad (2)$$

Also the area of ellipse would be, $A = \pi ab$ (3)

If we combine (1) and (2), we have :

$$a^2+b^2 = \frac{dX^2+dY^2}{4}$$

or $$(a+b)^2 = \frac{dX^2+dY^2}{4} + 2A/\pi$$

Let; $$Z^2 = (a+b)^2 = \frac{dX^2+dY^2}{4} + 2A/\pi \quad \text{or} \quad Z = a+b$$

Then:

$$b + A/\pi b = Z \quad \text{ie.,} \quad b^2 - Zb + A/\pi = 0$$

So that :

$$b = \left[Z - (Z^2 - 4A/\pi)^{\frac{1}{2}}\right]/2$$

$$a = Z - b$$

For finding position angle(ϕ), we can use the following equation:

$$dX = 2(a^2\cos^2\phi + b^2\sin^2\phi)^{\frac{1}{2}}$$

$$dX^2 = 4(a^2\cos^2\phi + b^2\sin^2\phi)$$

$$dX^2 = 4\left[a^2\cos^2\phi + b^2(1-\cos^2\phi)\right] = 4a^2\cos^2\phi + 4b^2 - 4b^2\cos^2\phi$$

Then :

$$4\cos^2\phi\,(a^2-b^2) = dX^2 - 4b^2$$

or :

$$\cos\phi = \left[\frac{dX^2 - 4b^2}{4(a^2 - b^2)}\right]^{\frac{1}{2}}$$

this equation gives an orientation between 0° and 90° .

N.B.1- In above discussion, we are not able to distinguish between positive and negative values of ϕ .

N.B.2- The equation for the axial ratio(b/a) has no solution when $Z^2 < 4A/\pi$ ie., when $\frac{dX^2 + dY^2}{2A} < 4/\pi$